Molecular Neurobiology (2019) 56:4620–4638
https://doi.org/10.1007/s12035-018-1378-0

The Exocyst Component Exo70 Modulates Dendrite Arbor Formation, Synapse Density, and Spine Maturation in Primary Hippocampal Neurons

Matías Lira[1] · Duxan Arancibia[1] · Patricio R. Orrego[1,2] · Carolina Montenegro-Venegas[3] · Yocelin Cruz[1] · Jonathan García[1] · Sergio Leal-Ortiz[4] · Juan A. Godoy[2] · Eckart D. Gundelfinger[3,5] · Nibaldo C. Inestrosa[2,6,7] · Craig C. Garner[8] · Pedro Zamorano[1,9] · Viviana I. Torres[2]

Received: 4 April 2018 / Accepted: 1 October 2018 / Published online: 29 October 2018

Abstract

Neurons are highly polarized cells displaying an elaborate architectural morphology. The design of their dendritic arborization and the distribution of their synapses contribute importantly to information processing in the brain. The growth and complexity of dendritic arbors are driven by the formation of synapses along their lengths. Synaptogenesis is augmented by the secretion of factors, like BDNF, Reelin, BMPs, or Wnts. Exo70 is a component of the exocyst complex, a protein complex that guides membrane addition and polarized exocytosis. While it has been linked to cytokinesis and the establishment of cell polarity, its role in synaptogenesis is poorly understood. In this report, we show that Exo70 plays a role in the arborization of dendrites and the development of synaptic connections between cultured hippocampal neurons. Specifically, while the overexpression of Exo70 increases dendritic arborization, synapse number, and spine density, the inhibition of Exo70 expression reduces secondary and tertiary dendrite formation and lowers synapse density. Moreover, increasing Exo70 expression augmented synaptic vesicle recycling as evaluated by FM4-64 dye uptake and the inverse was observed with downregulation of endogenous Exo70. Monitoring the formation of dendritic spines by super-resolution microscopy, we also observed that mRFP-Exo70 accumulates at the tip of EGFP-β-actin-positive filopodia. Together, these results suggest that Exo70 is essentially involved in the formation of synapses and neuronal dendritic morphology.

Keywords Neuron · Exocyst · Exo70 · Dendritic spine · Synapse · Dendrite

Electronic supplementary material The online version of this article (https://doi.org/10.1007/s12035-018-1378-0) contains supplementary material, which is available to authorized users.

✉ Pedro Zamorano
zamorano@gmail.com

✉ Viviana I. Torres
viviana.torres@gmail.com

[1] Departamento Biomédico, Universidad de Antofagasta, Antofagasta, Chile

[2] Departamento de Biología Celular y Molecular, Centro de Envejecimiento y Regeneración (CARE UC), Facultad de Ciencias Biológicas, Pontificia Universidad Católica de Chile, Santiago, Chile

[3] Department of Neurochemistry and Molecular Biology, Leibniz Institute for Neurobiology, 39118 Magdeburg, Germany

[4] Department of Materials Science & Engineering, Stanford University, Palo Alto, CA 94304, USA

[5] Center for Behavioral Brain Sciences and Medical Faculty, Otto von Guericke University, 39120 Magdeburg, Germany

[6] Center for Healthy Brain Ageing, School of Psychiatry, Faculty of Medicine, University of New South Wales, Sydney, Australia

[7] Centro de Excelencia en Biomedicina de Magallanes (CEBIMA), Universidad de Magallanes, Punta Arenas, Chile

[8] German Center for Neurodegenerative Diseases (DZNE), 10117 Berlin, Germany

[9] Instituto Antofagasta, Universidad de Antofagasta, Antofagasta, Chile

Introduction

Synaptogenesis is the process in which synapse contacts are established between neurons. Although it occurs throughout an entire lifespan, a rise of synapse formation is observed during early brain development [1] and this process is essential to create normal neuronal connectivity. Synapse formation is also thought to have a synaptotropic effect on the growth and elaboration of dendritic and axonal arbors [2, 3]. Filopodia extending from the surface of dendrites are dynamic structures that explore their environment seeking new synaptic partners, e.g., neighboring axons [4]. As such, they appear to play a fundamental role in the formation of synapses and dendritic spines both in vivo and in vitro [3, 5]. Mechanisms underlying synapse formation include intrinsic and extrinsic factors, as well as activity-dependent processes [6]. Dendritogenesis and synaptogenesis are thus believed to share overlapping mechanisms. For example, membrane trafficking, via small Rab-GTPases and SNARE proteins, is thought to contribute to the spatially restricted insertion of synaptic proteins (adhesion molecules, ion channels, and signaling receptors) at nascent synaptic contact sites [7–10]. Less well understood is the contribution of the exocyst complex to such processes.

The exocyst is an evolutionary conserved vesicle tethering protein complex that is formed by eight subunits: Sec5, Sec6, Sec8, Sec10, Sec15, Exo84, and two membrane-targeting subunits Sec3 and Exo70 [11]. During exocytosis and before SNARE-mediated vesicle fusion in yeast, the initial contact of secretory vesicles with the plasma membrane has been reported to depend on the exocyst [12, 13]. To date, the exocyst complex has been found to participate in a number of cellular processes, including cell division [14], polarized exocytosis and membrane growth [12, 15, 16], glutamate receptor trafficking [17, 18], and membrane targeting of the glucose transporter Glut4 [19]. In developing neurons, the exocyst has been localized to the tips of neurites and is required for neurite outgrowth [20]. Moreover, depleting Sec5 or the overexpression of dominant-negative Sec8 and Sec10 was shown to inhibit neurite enlargement in neurons and neuroendocrine PC12 cells [21, 22], consistent with a role in neurite formation. Recently, it has been reported that in *Drosophila* Sec6 interacts with Rop, the fly homolog of vertebrate Munc18-1, to regulate development of dendrites [23]. In *C. elegans* RAB-10 and the exocyst are necessary for dendritic arborization [24] and loss of Sec8 affects dendrite morphogenesis [25]. Similarly, in developing rat hippocampal neurons, it has been observed that Exo70 is required for axonal expansive elongation and axon regeneration [26, 27].

Exo70 can interact directly with the plasma membrane regions containing phosphoinositol-4,5-bisphosphate (PI(4,5)P2) through a phospholipid binding motif located in its C-terminus [28, 29], thereby mediating the targeting of the exocyst complex to the plasma membrane [30]. This has led to the hypothesis that Exo70 might be a nucleation factor for the assembly of the exocyst complex, establishing a contact between the component of the exocyst in the secretory vesicle (Sec 5, 6, 8, 10, 15, and Exo84) and the subunits present at the plasma membrane (Sec3 and Exo70). Additionally, Exo70 is the only exocyst subunit to induce filopodia formation in different cells types, including neurons, and has been shown to coordinate cytoskeleton and membrane trafficking by stimulating actin polymerization [31–33].

Taken together, the exocyst complex appears to be an important regulator of the morphogenic properties of cells. In the current study, we have examined whether Exo70 is a modulator of dendritic morphology and synaptogenesis of hippocampal neurons. Using gain and loss of function and imaging-based approaches, we find that Exo70 is an important regulator of dendritic branching, as well as the formation of dendritic spine and synapses between vertebrate hippocampal neurons.

Material and Methods

Antibodies

For Western blot, primary antibodies were mouse GFP 1:1000 (Roche, Germany), mouse Exo70 1:1000 (Santa Cruz, USA), mouse synaptophysin 1:500 (Santa Cruz, USA), mouse β-Actin 1:1000 (Sigma, USA), rabbit ERC2/ELKS2 1:500 (Synaptic Systems, Germany), and mouse HA 1:1000 (Covance, USA). Secondary antibodies were horseradish peroxidase-conjugated 1:10000 (Invitrogen, USA). Exocyst subunits mouse antibodies were used 1:500 (Santa Cruz, USA).

For immunofluorescence assays, primary antibodies were mouse HA 1:1000 (Covance, USA); rabbit Exo70 1:1000 (Proteintech, USA), mouse MAP2 1:1000 (Santa Cruz, USA), rabbit Piccolo 1:1000 (Synaptic Systems, Germany), rabbit Shank3 1:1000 (Synaptic Systems, Germany), and guineas pig Shank2 1:500 (Synaptic Systems, Germany). Mouse Bassoon 1:1000 (Synaptic Systems, Germany). Secondary antibody was highly cross-absorbed Alexa anti-rabbit, anti-mouse, and anti-guinea pig 1:1000 (Life Technologies, USA).

Plasmids and Lentiviral Vectors Constructions

The coding sequence of rat Exo70 (Accession no. NM_022691) was obtained by RT-PCR using total RNA isolated from rat brain. The forward primer Exo70 FP: 5′-ctcgaggcatgattcccccgcaggaggctt-3′ and the reverse primer Exo70 RP: 5′-gaattcttaagcagaggtgtcgaagagg-3′ were used to amplify the full-length ORF of Exo70. The PCR product was cloned into the pGEM-T plasmid (Promega), verified by

sequencing and subcloned into the XhoI/EcoRI sites of the bicistronic lentiviral vector pFUG-1D/2A-HA-W containing a HA epitope tag at the 5′ end of the cloning site [34] allowing the N-terminal tagging of the Exo70 construct (Fig. S1A). In order to obtain pFUR-Exo70-W construct, Exo70 full-length ORF was cloned into pmRFP-C1 using same *XhoI*/*EcoRI* sites. pFUG-W vector was digested with *AgeI* and *EcoRI* to eliminate EGFP ORF and then mRPF-Exo70 were subcloned into this construct using *AgeI*/*EcoRI* sites. Exo 70-directed short hairpin RNA (shRNA) was designed using previously described criteria [35–38]. Target rat sequence accession no. NM_022691 was used to design the shRNA oligonucleotides Exo70 shRNA FP: 5′-ctagc**ggaaccaagatttcatgaa**-caagaga**ttcatgaaatcttggttcc**ttttataat-3′ and Exo70 shRNA RP: 5′-tataaaaa**ggaaccaagatttcatgaa**-tctcttgaa**ttcatgaaatcttggttcc**g-3′. One hundred pmoles of each oligonucleotide was annealed in annealing buffer (100 mM potassium acetate, 30 mM HEPES and 2 mM magnesium acetate; pH 7.4) using a Thermocycler (Bio-Rad Laboratories). Annealed cDNAs were then phosphorylated using T4 polynucleotide kinase (New England Biolabs) and cloned as described previously [39] to obtain FUX-off shRNA plasmid (FUGW H1) and verified by sequencing.

Primary Hippocampal Neuronal Culture

Hippocampal cultures were prepared using a modified Banker's culture protocol described by Fernandez et al. [40, 41]. Briefly, hippocampi were dissected from embryonic Sprague-Dawley rats (E18). Neurons were dissociated with trypsin and plated at a density of 5.0×10^5 cells/cm^2 on poly-D-lysine (Sigma-Aldrich, USA)-coated coverslips in 12-well cell-culture dishes. Neuronal cultures were maintained in Neurobasal media supplemented with B27 (Gibco, USA), GlutaMAX-I (Gibco, USA), 100 U/ml ampicillin, and 100 μg/ml Streptomycin (Gibco, USA). Hippocampal neuronal cultures were maintained at 5% CO_2 at 37 °C. Half of the medium volume was changed weekly.

Lentiviral Production

HEK293T cells were transfected with the plasmids pCMVΔR8.9, pCMV-VSVg and the corresponding transfer vectors (pFUG-1D/2A-Exo70FL-HA-W, pFUG-1D/2A-HA-W, pFUG-Actin-W, pFUR-Exo70-W, pFUX-Off-W and pFUX-off[shRNA-Exo70]-W) to produce a functional lentivirus as described previously [42]. HEK293T cells were grown in DMEM supplemented with 10% fetal bovine serum and 100 U/ml ampicillin and 100 μg/ml Streptomycin (Gibco, USA). Lentiviral particles were collected from the supernatants at 24, 72, and 96 h, centrifuged, passed through a 0.45-μm filter and stored at − 80 °C. The viral titer was determined by fluorescence analysis of transduced HEK293T cells.

Transduction of Neuronal Hippocampal Cultures

Primary hippocampal neuronal cultures were infected on the day of preparation (0 DIV) with 100-μl aliquots of the lentivirus preparation, expressing EGFP and the HA-tagged Exo70 full-length ORF. As a control group, neurons were transduced with an EGFP only vector (FUG-1D/2A-HA-W). In spine formation/maturation experiments, 100-μl aliquots of mRPF-Exo70 and β-actin lentivirus were used to infect neuronal cultures on DIV 0 and DIV 1, respectively. For knockdown experiments using shRNAs, neurons were infected with the FUX-Off-W and FUX-off[shRNA-Exo70]-W lentiviral preparations. Neuronal cultures were fixed at the times indicated in the figure legends with LF fixative solution (60 mM PIPES, 25 mM HEPES, 10 mM EDTA, 2 mM $MgCl_2$, 0,12 M sucrose, 4% paraformaldehyde) for 10 min and then washed once with phosphate buffer saline (PBS) before processing for immunostaining.

Fluorescence Microscopy

After fixation, neurons were permeabilized with 0.5% (*v*/*v*) Triton X-100 in 1× PBS for 5 min and washed in 1× in PBS. Then, cells were incubated 30 min in blocking solution (2% Glycine, 2% BSA, 5% FBS, 50 mM NH_4Cl in PBS). To study dendrite morphology, neurons were stained with MAP2 and HA antibodies. Highly cross-absorbed Alexa-568 conjugated antibodies were used as secondary labels. Coverslips were mounted on slides with Vectashield (Vector Labs, USA) medium and images were captured in an Axiovert A10 Zeiss Microscope equipped with a Retiga-SRV camera (Q-Imaging) using Q-imaging software.

Confocal and Super-resolution Microscopy

Images to study synapse, dendrite, spine, and mRFP-Exo70 localization were acquired in an LSM780 NLO Zeiss and super-resolution Elyra S.1 (SR-SIM) microscopes both with the laser lines 488 and 561 nm and objective 63×, NA/1.4/WD 0.19 mm Plan-Apochromat Oil (CMA Bio-Bio, Universidad de Concepción). Confocal microscopy for endogenous Exo70, Shank2, Bassoon, and MAP2 immunostaining were performed in a Leica SP8 microscope, Objective 63× (Leibniz Institute for Neurobiology, Magdeburg). 3D reconstructions were performed by the Imaris software (CMA Bio-Bio). The density of cells per 18 mm coverslip was 50,000–60,000.

Immunoblot Analysis of Exo70 and EGFP in HEK293 Cells

Prior to homogenization, HEK293T cells were washed (twice) in ice-cold 1× PBS buffer containing Complete Protease Inhibitors Cocktail (Roche, Germany) and cells were removed

with a rubber policeman. Cells were lysed in homogenization buffer (10 mM HEPES, 1.5 mM $MgCl_2$, pH 7.4) and the protein concentration determined by Bradford assay. Proteins were separated in a 12% SDS-PAGE gel and transferred to a PVDF membrane (Hybond ECL membrane, GE Healthcare, USA). After transfer, the membranes were washed in 1× TBS-T (TBS 0.05% Tween 20) and blocked for 1 h in blocking solution (5% BSA, 3% milk, 1xTBS-T). After blocking, the blots were incubated with primary antibodies in TBS containing 3% FBS and 0.05% Tween-20 for 1 h at room temperature. After washing three times with 1× TBS-T, the membranes were blocked again for 1 h at room temperature and washed with 1× TBS-T. Then, the membranes were incubated with horseradish peroxidase-conjugated secondary antibodies (Invitrogen, USA) for 1 h at room temperature. After washing with TBS, the blots were developed using a chemiluminescence detection kit (ECL, GE Healthcare, USA). Images were obtained with an MF-ChemiBIS 2.0 Gel Documentation System (DNR Bio-Imaging System, USA).

Knock-down shRNA Cell Assay

The Exo70-directed shRNAs were assessed in HEK293T cells. Cultures at 50% of confluence were co-transfected with pFUR-Exo70-W, a plasmid expressing a mRFP-tagged Exo70, and pFUX-Off-W (Control) or pFUX-[shRNA EXO70]-W plasmids in a 1:5 ratio. Expression levels of Exo70 and actin were assessed after 72 h by Western Blot analysis.

FM Dye Uptake

To label functional neurotransmitter release sites, hippocampal neurons were infected with lentiviral vectors on day of plating and functional labeling of presynaptic boutons was performed with FM4–64 (N-(3-triethylammoniumpropyl)-4-(p-dibutylaminostyryl)pyridinium, dibromide) (Molecular Probes, USA) at 15 DIV as described [63]. Briefly, neurons were incubated in Tyrodes saline solution (119 mM NaCl, 2.5 mM KCl, 2 mM $CaCl_2$, 2 mM $MgCl_2$, 25 mM HEPES, 30 mM Glucose, buffered to pH 7.4) containing 15 μM FM 4–64. The cultures were then stimulated for 30 s at 10 Hz with 1 ms pulses, to load recycling vesicles sites with FM4-64, before washing cells with 1 mM ADVASEP 7 (β-Cyclodextrin Sulfbutyl Ether; Cydex, USA) for 1 min. Dye unloading was performed by stimulating the cultures with a second 30 s 10 Hz train. Images were obtained in load and unload conditions on a custom-built [39] scanning confocal microscope (Axiovert 100TV; Carl Zeiss, Inc., Germany) equipped with a 40 × 1.3 NA Plan Neofluar objective (Carl Zeiss, Inc., Germany) and 488 nm and 514 nm lasers (Sapphire 488-20CDRH and Compass 215 M-20; Coherent). FM dye uptake for Exo70-shRNA studies was performed as described [43].

Isolation of Subcellular Protein Fractions, Protein Quantitation, and Immunoblot Analysis

All manipulations were carried out on ice or at 4 °C. The forebrain was isolated from 12-week-old female Wistar rats and the fractionation was carried out as described by Smalla et al. [44]. Briefly, the forebrains were homogenized in buffer A (5 mM Hepes, pH 7.4; 320 mM sucrose) containing a protease inhibitor cocktail (ThermoFisher Scientific, Waltham, Massachusetts, USA) and phosphatase inhibitors (NaF, Na_3VO_4 and $Na_4P_2O_7$). The cell debris and nuclei were removed by centrifugation for 10 min at 1000*g* (P1 pellet), after that, the supernatant 1 (S1) was centrifuged for 20 min at 20,000*g* getting the supernatant 2 (S2) and pellet 2 (P2, crude membrane fraction). The P2 pellet was loaded on top of a 0.32/0.85/1.0/1.2 M sucrose gradient and centrifuged for 2 h at 100,000*g*. The fractions obtained from this first sucrose gradient included myelin (MY), light membrane (LM), or synaptosomes (S). For the isolation of synaptic vesicles (SV), synaptic membranes (SM), and postsynaptic densities (PSD), the synaptosomal fraction was divided into two equal fractions: one of them was submitted to osmotic shock with 5 volumes of 1 mM Tris-HCl pH 8.1 and stirring in an ice bath for 30 min, and then was loaded in the top of a 0.0/0.85/1.2 M sucrose gradient giving rise to SV and SM fractions. The other half of the synaptosomal fraction was submitted to Triton X-100 0.5% extraction and was loaded on the top of a 0.32/0.85/1.2/2.0 M sucrose gradient to isolate the PSD fraction. The presence of Exo70, synaptophysin and ELKS2/ERC2 in the different fractions was determined by immunoblot analysis.

Image and Statistical Analysis

The quantitative analysis of dendrite morphology was carried out with ImageJ (NIH) software with the assistance of the NeuronJ Plugin. All the dendrites from each neuron were quantified for parameters such as length, primary, secondary, and tertiary dendrite number. Quantitation of synaptic puncta was performed by visually counting puncta along three dendrites from each neuron. NeuronJ was used to measure the length of the dendrites, then synaptic density was calculated (Puncta/μm of dendrite). To quantify puncta intensity, OpenView 3 software [45] (provided by Noam Ziv) was used. Dendritic spine morphology categories (i.e., thin, mushroom and stubby) were determined using established parameters [46, 47]. Spine dimensions considered as follows: Thin, length 0.5–4.0 μm and bulb width 0.6 μm; mushroom, length 0.5–2.5 μm and bulb width 1.4 μm; stubby, length 1.0 μm and bulb width 1.0 μm. All data are expressed as the mean ± SEM,

the number of experiments is indicated in the corresponding figures. Difference between groups was determined Tukey's HSD analysis to establish significant differences. A $p < 0.05$ value was considered significant.

Results

Lentiviral Expression of Exo70

Exo70 is a subunit of the exocyst complex. While a role in axonal growth [20, 26] and the insertion of postsynaptic AMPA receptor has been described [18], the contribution of Exo70 to dendritic morphogenesis has not been investigated in detail. To explore this latter possibility, we overexpressed recombinant HA-tagged Exo70 in cultured hippocampal neurons via a bicistronic lentiviral expression system (Fig. S1a) [34]. The correct size protein expression was evaluated in HEK293T cells 48 h after transfection by immunoblot analysis (Fig. S1b). By placing the 1D/2A element between EGFP and HA-Exo70 in the bicistronic vector, we anticipated that cleavage would generate several protein species. Consistent with this concept, we observed a 26-kDa band immune-positive EGFP band, present in the constructs (Fig. S1b, left panel). We also observed a small amount of uncleaved protein, representing Exo70 domains fused to EGFP, and corresponding to Exo70FL (~98 kDa) (Fig. S1b, left panel). As Exo70 is HA-tagged at the N-terminus, it was also possible to detect it in Western blot with HA antibody (Fig. S1c). The construct expressed the protein of the expected size, Exo70FL (~ 72 kDa) (Fig. S1b, right panel). The maximum transduction efficiency expressed as the percentage of neurons transduced with the lentiviral vector was on average 90% (Fig. S1c). We did not observe any decrease in the number of transduced neurons during the time in culture (data not shown).

Hippocampal neurons were infected with the Exo70 lentiviral construct on the day of plating and fixed on day in vitro (DIV) 15. Infected cells were identified by the expression of EGFP that filled most of the neuronal perikaryon and neurites (Fig. 1a, left panel). Staining of these cells with HA antibody revealed a slightly punctuated pattern mainly along membranes for Exo70FL with some diffuse localization within neurites and filopodia-like structures (Fig. 1a, gray images). The control vector, expressing only the HA tag, showed only a very modest fluorescence staining with the HA antibody, likely due to a rapid degradation of the peptide (Fig. 1a, gray images). Interestingly, monitoring cell morphology of DIV 7 neurons exploiting the soluble EGFP signal revealed a significant increase in filopodia along neurites (most likely dendrites) from cells co-expressing HA-Exo70FL (Fig. 1b, c). These results agree with previous reports in several cells lines [33, 48, 49], where the expression of the Exo70 induces the formation of filopodia-like structures.

Expression of Exo70 Modulates Dendritic Branching

In addition to the increase in filopodia, neurons overexpressing HA-Exo-70FL appeared to exhibit an increase in dendritic branching (Fig. 1b), a phenotype not previously reported. To explore this further, we analyzed several dendritic parameters, including the number of primary, secondary, and tertiary dendrites in neurons overexpressing the Exo70 construct. This was accomplished by imaging DIV 15 neurons after fixation and staining with the dendritic microtubule-associated protein 2 (MAP2), a highly specific somatodendritic marker (Fig. 2a). In transduced EGFP-positive cells, the number of secondary (HA 7.0 ± 0.35, FL 11.5 ± 1.0) and tertiary dendrites (HA 1.05 ± 0.31, FL 3.15 ± 0.37) but not primary dendrites were affected by the overexpression of Exo70FL compared to their respective controls (Fig. 2b). Both the length as the proportion of primary dendrites were not affected by the overexpression of Exo70FL (Fig. 2c); however, the same parameters were increased in the case of secondary dendrites when compared to the control (length: HA 25.35 ± 3.45, FL 34.85 ± 21.15; proportion: HA 0.15 ± 0.04, FL 0.29 ± 0.04; $p < 0.005$) (Fig. 2d). This indicates that the effect of Exo70FL on dendritic arborization specifically affects higher order branching of dendrites. To assess whether these effects were restricted to proximal or distal dendrite branching, a Sholl analysis [50] was performed to monitor changes in the dendritic tree. The analysis revealed that overexpression of Exo70FL leads to a significant increase of intersections, and hence dendrite numbers, within a distance of 20–45 μm to the cell soma as compared to controls (Fig. 2a, right panel).

The changes induced by Exo70FL in the number of secondary and tertiary dendrites could be seen at an earlier stage, i.e., DIV 7 (Fig. S2a, b). This suggests that initial effects of Exo70 overexpression on secondary and tertiary dendrites act already in immature neurons. At this stage, primary dendrite length (HA 38.85 ± 2.65; FL 42.11 ± 2.90) and number (HA 5.30 ± 0.30; FL 5.47 ± 0.33) did not change (Fig.S2b, c). A significant increase in secondary dendrite number (HA 4.00 ± 0.28; FL 6.63 ± 0.59, b, c) $p < 0.01$) and tertiary dendrite number (HA 0.44 ± 0.14; FL 1.15 ± 0.25, $p < 0.05$) was observed (Fig. S2b). A Sholl analysis shows that the complexity of dendrites increases slightly (Fig. S2a, graph).

As the overexpression of Exo70FL in hippocampal cultures affects dendritic branching, we asked whether loss of function experiments would have an opposite effect. To address this, we generated a short hairpin RNA (shRNA) that reduced expression of Exo70 by approximately 50% in HEK293T cells (Fig. 3b). We transduced neurons at DIV 0 with a lentivirus vector containing the Exo70 shRNA and that also expresses EGFP and analyzed them at DIV 15 by staining for MAP2 after fixation (Fig. 3a). Sholl analysis shows that a reduction of endogenous Exo70 produces a decrease of intersections in dendrites beyond 45 μm (Fig. 3c). Interestingly,

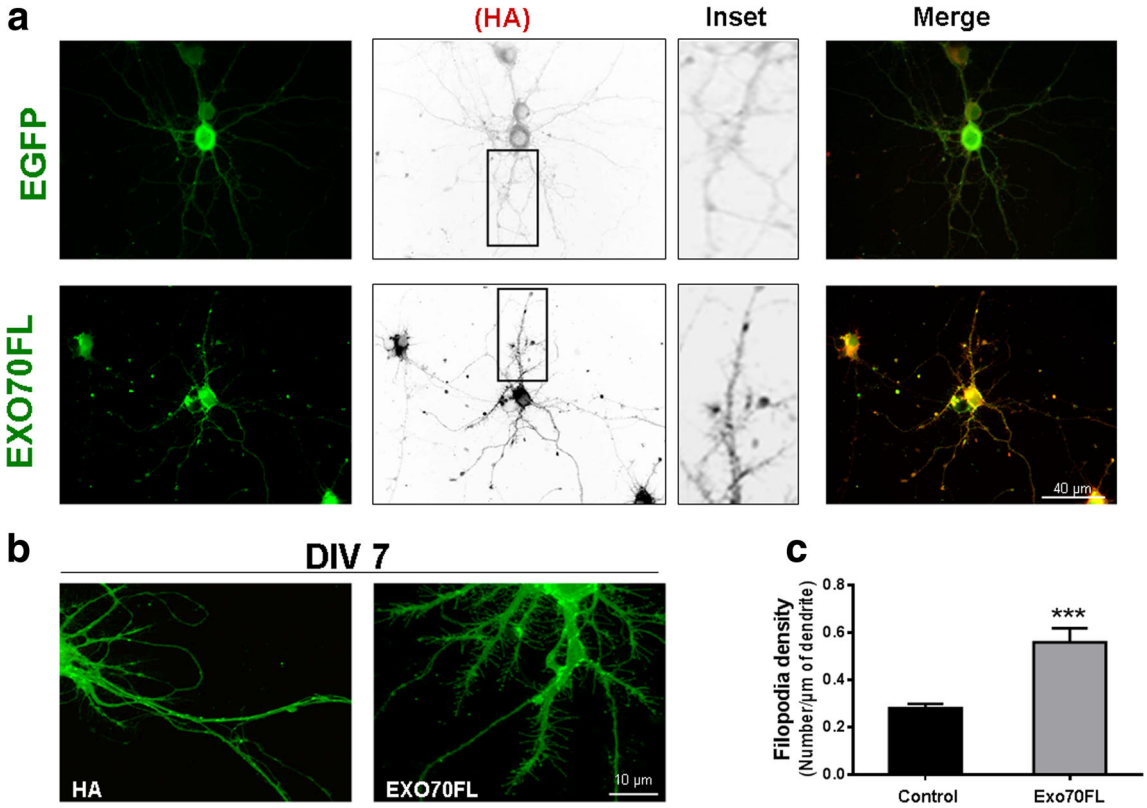

Fig. 1 Characterization of Exo70FL expression by lentiviral vectors in rat hippocampal neurons. **a** Rat hippocampal neurons were transduced at the day of plating (0 DIV) with bicistronic lentivirus expressing EGFP and Exo70FL, fixed at DIV 15 and immunostained with HA antibody. Exo70FL displays a discontinuous membrane staining pattern in neurites and is present in filopodia. Insets are magnifications of boxes indicated in HA staining. **b** Representative images showing EGFP expression on neurites section of cultures fixed at DIV 7. An increase in filopodia formation is observed in neurons transduced at DIV 0 with the Exo70FL lentivirus. **c** Quantitative analysis of filopodia density induced by overexpression of Exo70FL. Each experimental group considered 2 independent experiments. Values represent means ± SEM, $n = 15$ neurons per experiment, $^{***}p < 0.005$

neurons expressing Exo70-directed shRNA showed 33% ($p < 0.05$) and 50% ($p < 0.005$) decrease in the number of secondary and tertiary dendrite, respectively (Fig. 3d). No effect on primary dendrite number was observed (Fig. 3d). Primary dendrite length was decreased by 23% ($p < 0.005$) compared to neurons transduced with the control virus, while the number of primary dendrites that branch remained unchanged (Fig. 3e). In neurons expressing Exo70 shRNA secondary dendrite length and branching was decreased by 37% ($p < 0.005$) and 33% ($p < 0.05$), respectively (Fig. 3f). These results show that inhibition of Exo70 expression induces the opposite effect seen in the overexpression experiments and suggest that the regulation of Exo70 expression plays an important role in modulating dendritic branching during neuronal development.

The exocyst complex was first described as an octameric complex working as a whole in several basic cellular functions; however, some subunits have been related to specialized functions as is the case of Exo70. It could be thought that by altering the expression of an exocyst subunit the expression of another component could be affected and, therefore, the change in the dendritic/spine structure observed after modifying Exo70 levels could be a consequence of the alteration of the levels of another subunit. To explore this possibility, we evaluated whether overexpression of Exo70 alters the expression levels of other exocyst subunits (Fig. S3). We overexpressed GFP-Exo70 in HEK293T cells and analyzed the expression of several exocyst subunits by Western blot. The presence of GFP-Exo70 and endogenous Exo70 was evaluated with a specific antibody (Fig. S3b). The overexpression of GFP-Exo70 is clearly visible and is overexpressed several folds in comparison with the endogenous Exo70 (Fig. S3b). This overexpression results in a change on the phenotype of the transduced cells, showing an increase in lamellipodia and filopodia as expected (Fig. S3a, inset). The increase in Exo70 expression and the change in the cell phenotype did not alter the expression levels of Sec5, Sec6, Sec8, and Sec10 subunits as analyzed by Western blot (Fig. S3c), suggesting that Exo70 does not modulate the expression of the others Exocyst subunits.

To verify the specificity of the effect observed with the overexpression of Exo70 on the dendritic tree, we overexpressed Sec5 and Sec6 subunits in hippocampal neurons. Figure 4a shows two neurons DIV 15 stained with

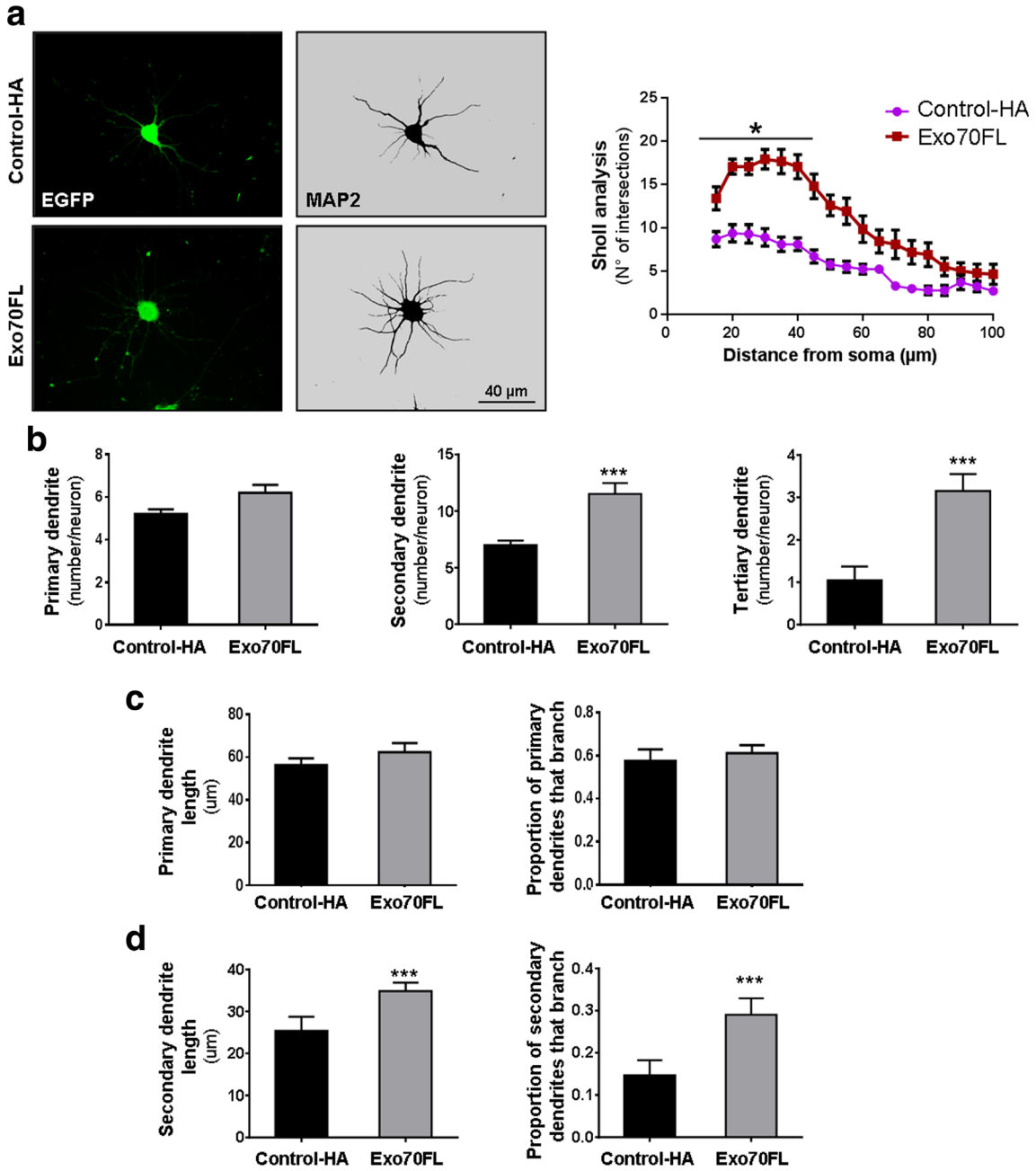

Fig. 2 Expression of Exo70FL modulates changes in dendritic arborization in hippocampal neurons. **a** Rat hippocampal neurons were transduced at the day of plating (0 DIV) with bicistronic lentivirus expressing EGFP and Exo70FL, fixed at DIV 15 and immunostained for MAP2. Sholl analysis was performed to show the degree of arborization. Dendritic parameters were quantified as: **b** number of primary, secondary and tertiary dendrites. **c** Length primary dendrites and proportion of primary dendrites that branch. **d** Length of secondary and proportion of secondary dendrites that branch in hippocampal neurons. Each experimental group included 3 independent experiments. Quantification was made in binary saturated MAP2 immunofluorescence images using ImageJ. The quantification was carried out on all dendrites per neuron. Values represent means ± SEM, $n = 20$ neurons per experiment. *$p < 0.05$, ***$p < 0.005$

MAP2, transfected with Sec5 or Sec6 (green fluorescence). The dendritic tree was compared between transfected and non-transfected neurons within the same coverslip. The analysis of Sholl shows that Sec5 and Sec6 expression did not affect the complexity of the dendritic tree (Fig. 4a, graph), and neither of these two subunits affected the length and number of primary dendrites, nor the number of secondary dendrites (Fig. 4c, d). These findings confirm a specific effect of Exo70 on hippocampal neuron dendritic arborization.

Presence of Exo70 in Synaptic Compartments

Exo70 is a subunit of the exocyst complex that associates to membranes through lipid-binding motifs [28]. This is in

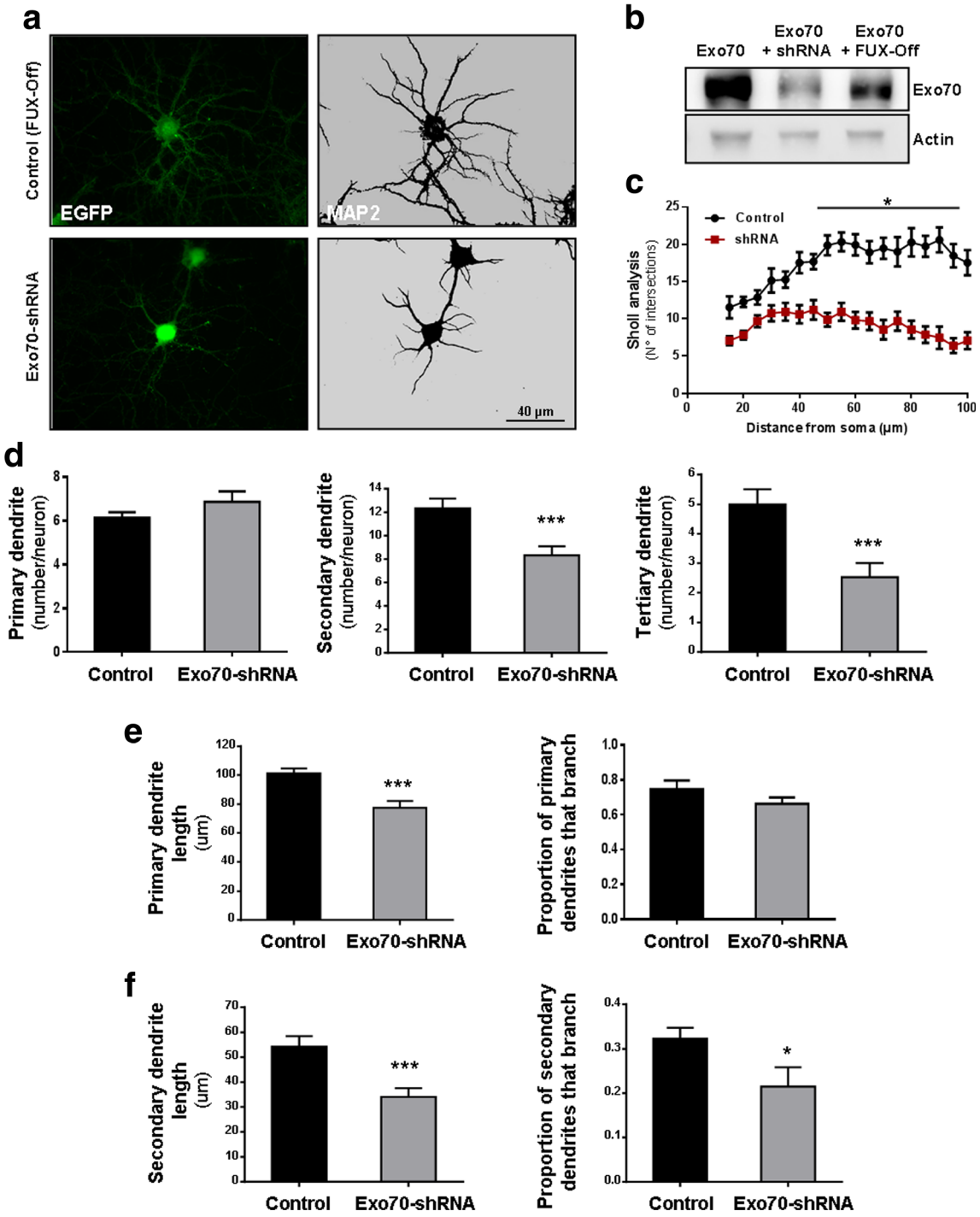

Fig. 3 Reduction of endogenous Exo70 expression reduces primary and secondary dendrite length, and number of secondary dendrites. **a** Rat hippocampal primary neurons were transduced with lentivirus containing Exo70-directed shRNA and control vector (FUX-Off) at DIV, 0 fixed at DIV 15 and immunostained for MAP2. **b** Knock-down assay in HEK-293T cells transfected with Exo70-directed shRNA. Co-transfected rat mRFP-tagged Exo70 was evaluated and shows a reduction of the endogenous protein by ~ 50% as evaluated by immunoblot analysis. **c** Sholl analysis was made to show the degree of arborization due to the decrease of Exo70 protein by Exo70-shRNA. Dendritic parameters were quantified as **d** number of primary, secondary, and tertiary of dendrites, **e** length primary dendrites and proportion of primary dendrites that branch, **f** length of secondary dendrites and proportion of secondary dendrites that branch. Each experimental group included 2 independent experiments. Quantification was made in binary saturated MAP2 immunofluorescence images using ImageJ. The quantification was carried out on all the dendrites per neuron. Values represent means ± SEM, $n = 15$ neurons per experiment. *$p < 0.05$, ***$p < 0.005$)

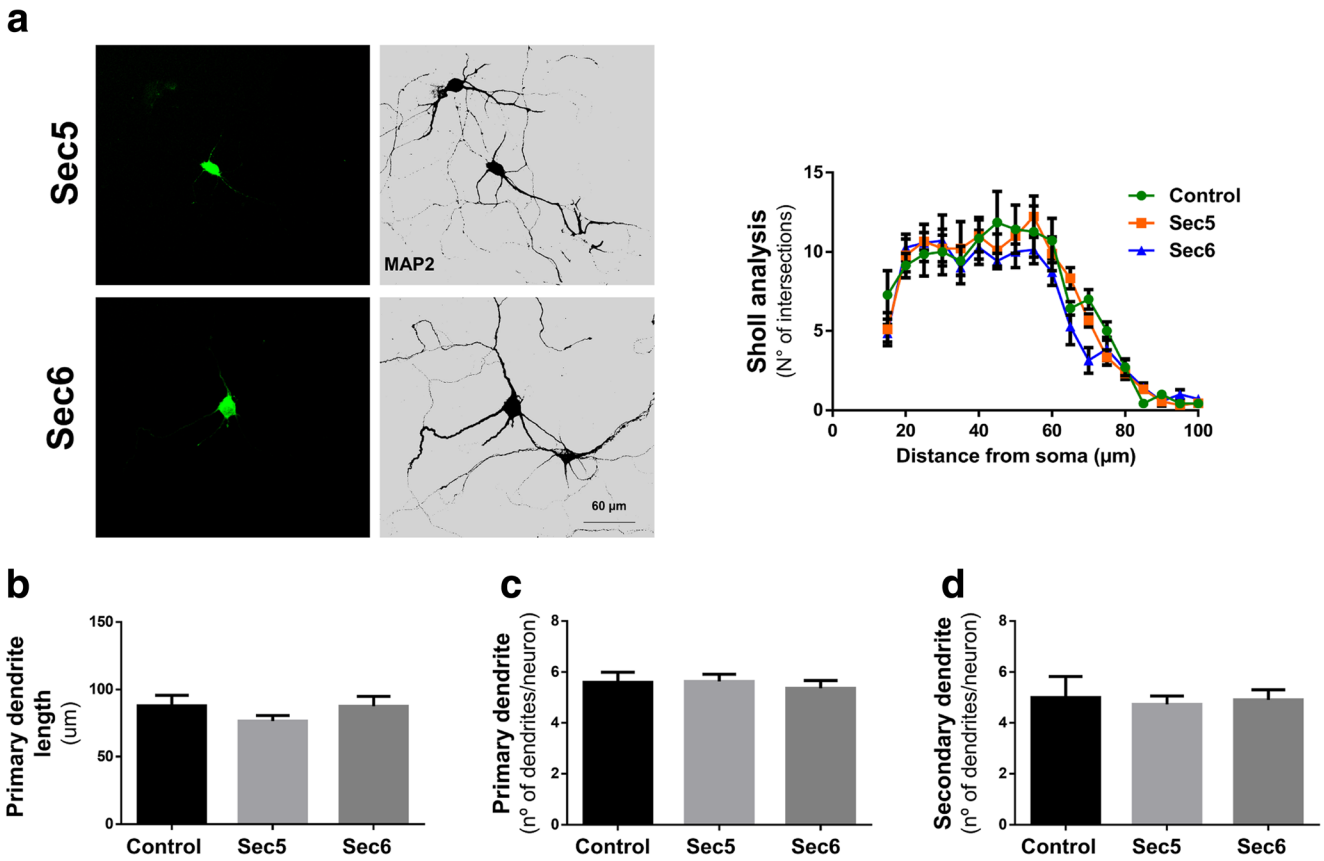

Fig. 4 Overexpression of Sec5 and Sec6 did not affect dendrite arbor. **a** Rat hippocampal neurons were transfected either with Sec5 or Sec6 and fixed a 15 DIV and immunostained for MAP2. Sholl analysis was performed to determine dendritic arbor complexity. **b** Primary dendrite length. **c** Primary dendrite density. **d** Number of secondary dendrites. Values represent means ± SEM, $n = 10$ neurons per experiment

accordance with a role in the addition of membranes during dendritogenesis. Previous studies have observed components of the exocyst in axons and dendrites and associated with the insertion of AMPA-type glutamate receptors at the postsynaptic membrane [18]. As synaptogenesis is tightly coupled to dendritic arborization [51], it is conceivable that the exocyst and Exo70 contribute to dendritogenesis by influencing synapse formation. As an initial test of this hypothesis, we examined whether Exo70 biochemically associates with synaptic junctional protein preparations. This was accomplished by Western blotting of biochemically fraction at brain membranes [44, 52]. Data presented in Fig. 5 shows that Exo70 is present in synaptosomes (SYN), synaptic membranes (SM), as well as in purified postsynaptic density protein (PSD) fractions. A dim band is observed in the synapse vesicle fraction, and its strong presence in SM and PSD fractions suggests that Exo70 is associated with synaptic junctions. Gradient performance was controlled by assessing the distribution of the presynaptic proteins ERC2/ELKS2, an active zone scaffolding protein, and synaptophysin, a synaptic vesicle (SV) protein which were distributed as expected (Fig. 5).

Since these biochemical experiments do not distinguish between proteins associated with the pre or postsynaptic side of the synaptic junction, we used immunocytochemistry to examine the spatial distribution of Exo70 in cultured hippocampal neurons at DIV 21. As described previously [18] antibodies against Exo70 revealed a punctate staining pattern along MAP2 positive on dendrites (Fig. 6). Many of the Exo70 positive puncta exhibited a spiny pattern along dendrites that occasionally were situated juxtaposed to Bassoon puncta (Fig. 6a; yellow arrowheads) and did colocalize with Shank2 (Fig. 6b; yellow arrow), suggesting a postsynaptic localization Exo70. Consistent with this conclusion, a 3D reconstruction of several spiny synapses using Imaris software revealed that endogenous Exo70 (Fig. 6c) co-localized with the PSD protein Shank2 in dendritic spines, while recombinant mRFP-tagged Exo70 became localized in the spine heads of β-actin stained dendritic spines (Fig. 6d). Although less obvious, we also detected Exo70 along MAP2 negative processes that co-localized with Bassoon, consistent with an axonal distribution at an orphan synaptic site or inhibitory synapses (Fig. 6a, white arrows). Together, these data are consistent with a presence of Exo70 at excitatory synapses and dendritic spines.

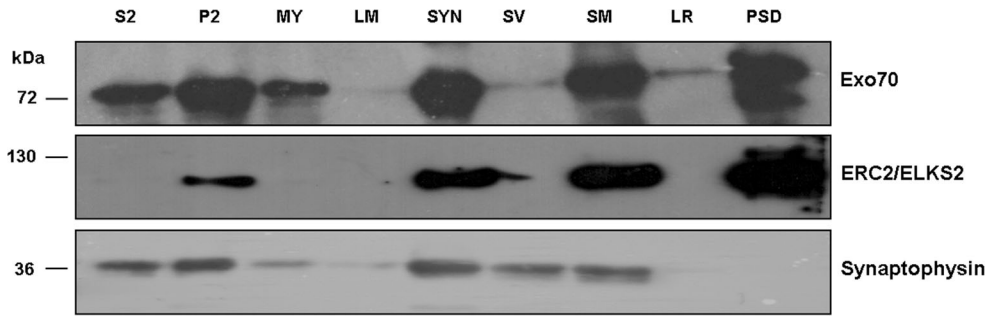

Fig. 5 Endogenous Exo70 is associated to synapse junctions. The brains from 12 weeks-old rats were fractionated by differential centrifugation (see methods). Equivalent volumes of samples from each fraction were loaded in order to determine molecular distribution of Exo70 protein. Distribution of Exo70, the presynaptic scaffolding protein ERC2/ELKS2 and the synaptic vesicle marker synaptophysin in the different brain fractions. S2: supernatant 2; P2: pellet 2; MY: myelin; LM: light membrane; SYN: synaptosomes; SV: synaptic vesicles; SM: synaptic membranes; LR: lipid raft; PSD: postsynaptic density

Expression of Exo70 Modulates Synapse Formation

To investigate whether the increase in complexity of dendrite morphology induced by Exo70 is accompanied by an increase in synapse formation, we overexpressed Exo70 in hippocampal neurons transduced the day of plating and analyzed the effect on the number and distribution of synapses identified either with antibodies against Piccolo, a presynaptic active zone marker (Fig. 7a), or the postsynaptic marker Shank3 (Fig. 7b) at DIV 15. Quantifying the number of Piccolo positive puncta per μm of dendrites revealed a ~1.8-fold, increase in puncta density in Exo70FL-expressing neurons compared to HA control (Fig. 7a; HA 0.39 ± 0.02/μm, Exo70FL 0.71 ± 0.03/μm; $p < 0.005$). When we tested for the postsynaptic marker Shank3, we also detected a ~ 1.5-fold increase in puncta density (Fig. 7b, e; HA 0.49 ± 0.01/μm, Exo70FL 0.72 ± 0.04/μm; $p < 0.005$). To assess changes in synapse size, we analyzed changes in the puncta intensity of Piccolo or Shank3-positive puncta. Here, we observed a small but significant increase in the average Piccolo puncta fluorescent intensity upon Exo70FL overexpression (Fig. 7a). Conversely, the overexpression of Exo70FL had no significant effect on Shank3 puncta fluorescent intensity (Fig. 7b).

Next, we asked whether down-regulating the expression of endogenous Exo70 would affect the synapse number. As expected, knock-down of Exo70 with a specific shRNA not only reduced the number of Piccolo puncta per length of dendrites (by ~ 34%) (Fig. 7c), but also the fluorescence intensity per putative presynaptic bouton (by ~ 20%) (Fig. 7c). These results suggest that Exo70 plays a role in the formation and/or stability of hippocampal synapses.

Exo70 Overexpression Increases the Number of Functional Presynaptic Release Sites

The ability of Exo70 to modulate the intensity of Piccolo puncta suggests that it might also influence the docking, fusion and recycling of SVs within presynaptic boutons. To explore this possibility, we measured the density of recycling sites of SVs utilizing the styryl dye FM4-64 [53] at boutons of neurons expressing Exo70FL or HA alone (Fig. 8a). First, we explored the efficiency of SV exocytosis. Boutons of control neurons and neurons expressing Exo70FL loaded with FM4-64 were stimulated for 30s at 10 Hz and the fraction of released FM4–64 dye/puncta was measured. Boutons overexpressing Exo70FL displayed enhanced exocytosis (5.75 ± 0.19) compared to control boutons (4.30 ± 0.40) (Fig. 8a). Also, the density of FM4–64 positive puncta increased significantly with the expression of Exo70FL (1.0 ± 0.22/μm) compared with control (0.55 ± 0.07/μm) (Fig. 8a). This suggests that the increased number synaptic puncta observed in Fig. 7 are likely to reflect active synapses.

When expression of endogenous Exo70 was downregulated, we observed a dramatic decrease in the efficiency of the FM dye discharge (Fig. 8b) suggesting a specific role of Exo70 in the presynaptic terminal. This together with the presence of Exo70 in the presynapsis (colocalization with Bassoon, Fig. 6a white arrows) and the increase of the FM load/unload ratio observed with the Exo70 overexpression, suggests a role of this subunit of the exocyst in the efficacy of the release of the synaptic vesicles. It will be interesting to investigate at what level of the synaptic vesicle cycle this protein is participating; however, this is beyond the scope of this article.

Exo70 Overexpression Increases Dendritic Spine Density and Induces a More Mature Spine Phenotype

Excitatory synapses are often formed on the tips of dendritic spines, small protrusions present along the length of neuronal dendrites. As Exo70FL was observed to increase the number of functional synapses, it was of interest to examine whether it also influenced the maturation and morphology of dendritic spines. This was accomplished by co-infecting neurons with two lentiviruses: one expressing EGFP-β-Actin to visualize the spines and the second

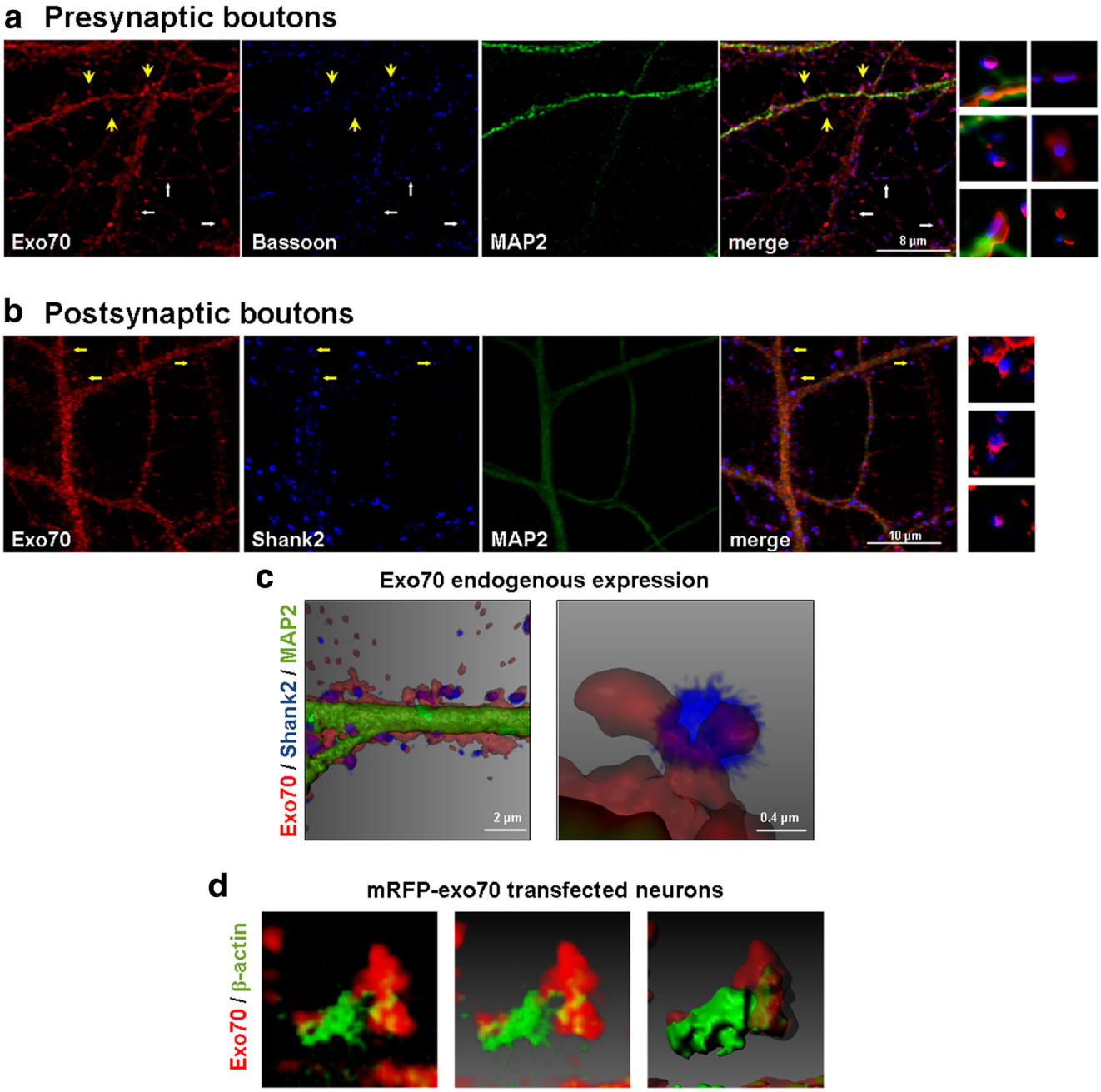

Fig. 6 Endogenous Exo70 is found in both pre- and postsynaptic compartments. Rat hippocampal neurons were fixed at DIV 21 and immunostained for **a** Exo70, the presynaptic marker Bassoon and the dendritic marker MAP2, or **b** Exo70, the postsynaptic density protein Shank2 and MAP2. Exo70 co-localized with Bassoon in MAP2 free neurites (white arrows), and on structures that appear to be dendritic spines aligned with Bassoon-positive presynaptic boutons (yellow arrowheads) in (**a**). Yellow arrows in (**b**) show co-localization of Exo70 with Shank2. **c** 3D-reconstruction and blend projection of confocal images of endogenous Exo70, Shank2 and MAP2. **d** 3D-reconstruction of mRFP-Exo70 and β-actin of images acquired by super-resolution microscopy

expressing mRPF-Exo70FL at the day of plating. Neurons were then fixed at DIV 21 (Fig. 9a) representing a relatively mature stage of neuronal development. Consistent with an increase in synapse number (see Fig. 7a, b), we observed that mRFP-Exo70FL significantly increased the density of dendritic spines (0.69 ± 0.02/µm) compared to control (0.57 ± 0.02/µm) ($p < 0.005$) (Fig. 9c).

During development, spinogenesis proceeds from initially small filopodia-like appearance to more mature, i.e., stubby and mushroom-shaped morphology. Our analysis of EGFP-Actin/mRFP-Exo70FL expressing neurons revealed that Exo70FL overexpression decreased the density of filopodia (control, 0.34 ± 0.01/µm; Exo70FL, 0.10 ± 0.01/µm) (Fig. 9d) as well as the average spine length (control, $1.85 \pm$

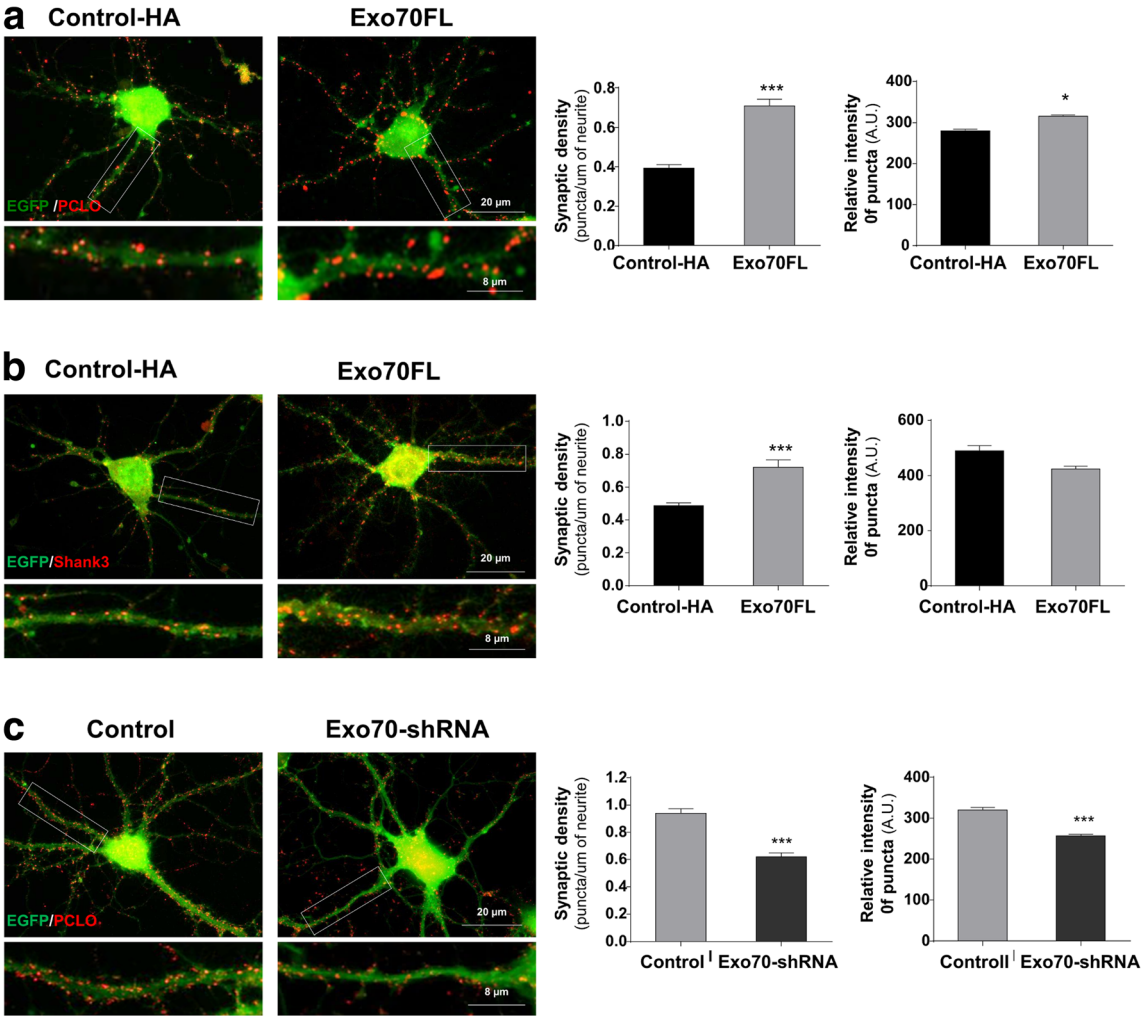

Fig. 7 Overexpression and downregulation of Exo70 alters synapse density in hippocampal neurons. **a**, **b** Representative images showing EGFP expression and immunostaining for synaptic marker proteins. Neuronal cultures were transduced with bicistronic lentivirus expressing Exo70FL at 0 DIV and fixed at DIV 15. Neurons were immunostained for **a** Piccolo and **b** Shank3 to visualize pre- and post-synaptic sides, respectively. Bottom panels correspond to magnifications of dendrite sections marked in upper panels. Synaptic density was quantified in primary dendrites with $n = 20$ neurons. Synaptic puncta intensity quantification was carried out in three primary dendrites per neuron with OpenView3 software. $n = 10$ neurons per experiment. Each experimental group included 3 independent experiments. Values represent means ± SEM. $*p < 0.05$, $***p < 0.005$. A.U.: arbitrary units. **c** Neuronal cultures were transduced with lentivirus expressing EGFP and Exo70-directed shRNA and EGFP at DIV 0 and fixed at DIV 15. Representative images showing EGFP expression and Piccolo staining. Lower panels; magnifications of dendrite sections boxed in the above panel. Synaptic density was quantified in 3 primary dendrites per neuron, $n = 15$ neurons. Synaptic puncta intensity quantification was carried out in total dendrite number per neuron. $n = 10$ neurons per experiment. Each experimental group included 2 independent experiments. Values represent means ± SEM, $***p < 0.005$. A.U.: arbitrary units

0.05 μm; Exo70FL 1.39 ± 0.09 μm) (Fig. 9e), whereas the width of the spine heads significantly increased (control, 0.64 ± 0.07 μm; Exo70FL, 0.94 ± 0.07 μm) (Fig. 9f). These observations agree with the assumption that Exo70 promotes the maturation of spines.

We analyze more thoroughly filopodia/spines development by studying and comparing the number of filopodia and spines in stages DIV 7, 15 and 21 in neurons overexpressing Exo70FL. In Fig. 10a are represented neurons transduced with the bicistronic lentivirus containing GFP (pseudocolor in gray) and Exo70FL. Quantification of filopodia and spines shows that in control neurons filopodia increases with the aging culture and decrease in cultures overexpressing Exo70FL (Fig. 10b). The number of spines increases in both cases with the age of the culture but there is a higher density of spines in DIV 15 and DIV 21 in neurons that overexpress Exo70 compared to the control. These results suggest that Exo70 induces early maturation of the spines, probably due to the higher density of filopodia observed between DIV 7–15 with overexpression of the protein, but also the overexpression of Exo70 results in more spines as seen in DIV 15 and 21 compared to control neurons.

Interestingly, Exo70 seems to be located primarily at the tip of the filopodia and spines throughout spinogenesis (Fig.S4). For example, in representative epifluorescence images, mRPF-Exo70FL was observed at the tip and along the shafts of filopodia at DIV 7 and DIV 11 (Fig. S4). Likewise, mRPF-Exo70FL accumulated in the head of mature dendritic spines in DIV 21 neurons (Fig. S4). Analysis by super-resolution microscopy revealed that mRPF-Exo70FL is indeed located predominantly at the tip of filopodia and within the spine heads of mushroom and stubby spines (Fig. 11a–d) consistent with a role for Exo70 in synaptogenesis and maturation of dendritic spines.

Discussion

The exocyst complex basic function is the tethering of secretory vesicles during the process of membrane addition for polarized outgrowth [54], and its protein components have been involved in specialized membrane processes in neurons, mainly in invertebrates. Here, we report on a more general role of the exocyst and in particular Exo70 during dendritogenesis, synapse and spine formation. We show that in the rat brain Exo70 distributes with major synaptic protein fractions (Fig. 5). Therefore, we performed experiments aimed to modulate the expression of Exo70 and evaluate its effect on neuronal maturation including dendrite branching, and synapse formation and spine maturation. To this end, we employed an overexpression and a knock-down strategy for Exo70 in primary hippocampal neurons taking advantage of a third-generation full-length HA-tagged Exo70. Lentiviral-mediated protein expression in cultured neurons by itself results in low and constant expression and, more importantly, it does not affect network activities [55]. Our results suggest that not only is Exo70 expressed during early stages of neuronal morphogenesis within dendrites and synapses, but also seems to play an active role in the arborization of dendrites, spine morphogenesis and synapses formation, consistent with a dynamic role for this exocyst component during the entire neuronal development.

Exo70 and Dendrite Branching of Hippocampal Neurons

In the present work, we show that Exo70 overexpression increases the number of secondary and tertiary dendrites. Conversely, inhibition of Exo70 expression by shRNA resulted in a reduction of dendrite length, including primary dendrites. The fact that no effect is observed on primary dendrites upon overexpression of Exo70, might be due to the relatively slow onset of expression accomplished by the lentivirus system. In neurons transduced at the day of plating, EGFP expression usually is not observed before 3 DIV, a period that coincides with the formation of the first neurites in hippocampal neuron cultures as they transition from stage two to stage three neurons [41]. A role in primary dendrite formation of Exo70 seems to be unmasked upon attenuation of Exo70 expression via shRNA knock-down of Exo70. Though also here a lentivirus system is used, small constructs of shRNA may be expressed much faster than FL-proteins. This would suggest a critical time window for Exo70 action on primary dendrite branching during the very first days in culture.

To the best of our knowledge, there is no report in mammalian neurons involving the Exo70 protein in dendrite arborization. However, several subunits of the exocyst complex (Sec5, Sec6, and Sec8) have been linked to dendritic growth and patterning in invertebrates [23, 25]. In sensory PVD neurons of *C. elegans*, the exocyst complex was proposed to act as an effector of the GTPase Rab10 promoting docking and fusion of secretory vesicles during dendrite growth and branching [25]. In *Drosophila* class IV neurons, the knockdown of Rab10 and Exo84 induced a reduction in the dendritic arbor [25]. Intriguingly, knockdown of Rab10, and two Exo70 interactors, Sec8 or Exoc84, did not alter dendrite length in cultured rat hippocampal neurons but did lead to a dramatic reduction in the density of dendritic spines at 21 DIV [25]. Also, in *Drosophila*, a role was given to the exocyst complex in the development of dendrites of C4da neurons which elaborate highly complex dendritic arbors [23]. In that study Ras opposite (Rop), the *Drosophila* ortholog of mammalian Munc18-1, mediated dendrite growth together with the exocyst subunit Sec5 and Sec6. Both Rop and the exocyst proteins were mostly found in primary dendrites, where exocytosis was the main mechanism of membrane outgrowth driven for these proteins. The authors postulated that terminal dendritic growth most probably depends on the diffusion of material from primary dendrites [23].

In vertebrates, many molecules of diverse function have been described to have a role in the growth and arborization of dendrites [56]. These proteins include regulators of transcription [57, 58], secreted proteins [59–63], regulators of cytoskeletal dynamics [64–66], motor proteins [61, 67], and proteins of the secretory pathway and endocytic pathway [68, 69]. In these last studies it was reported that the addition of lipids and proteins through exocytosis is fundamental for the growth of dendrites. In the case of Exo70, there is only one report in hippocampal neurons where this exocyst subunit participates in membrane expansion at the axonal growth cone [26]; however, a role in dendrite arbor as mentioned above has not been explored. Therefore, we are the first to report a role of the Exo70 exocyst subunit in dendrite growth and branching.

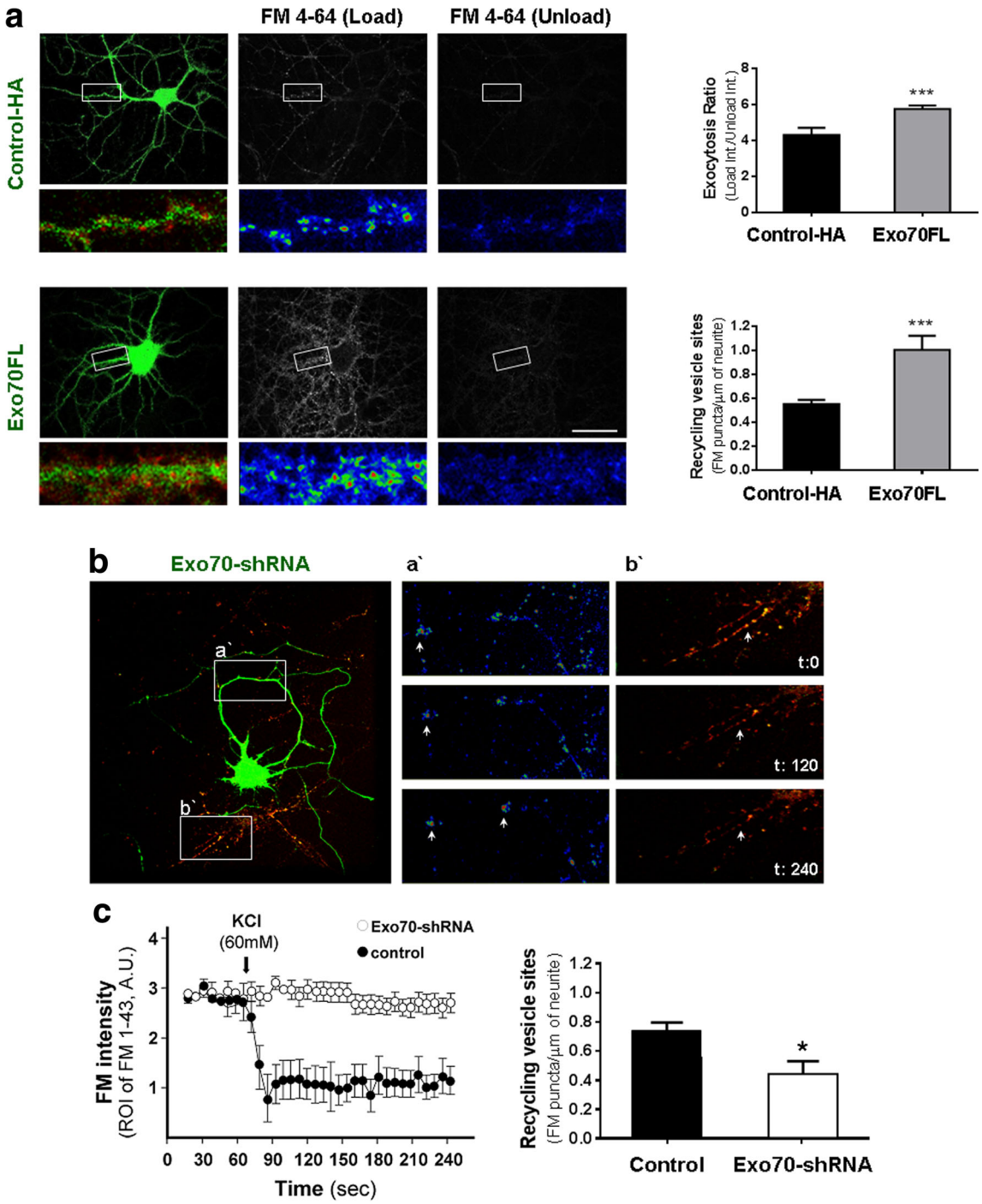

Exo70 and Dendritic Spines Density and Maturation

In young cultures, we observed that Exo70 overexpression induces filopodia formation. Since filopodia are the precursors of dendritic spines, we decided to study Exo70 role on these neuronal protrusions. The maturation of dendritic spines has been extensively studied [70–73]. Shortly after initial axo-dendritic contact, PSD-95 clusters emerge in motile filopodia triggering its retraction to form a protospine that stabilizes the nascent synapse [70]. This transition is seen in P4 juvenile rats where synapses are forming. Thus, retraction of filopodia is the process that neurons use to form excitatory synapses on dendritic spines. Generally, filopodia are described as antennas that cells use to explore their microenvironment, and in neurons, it has been observed that filopodia have a role in synaptogenesis [5]. In addition, Sekino and colleagues proposed that filopodia are essential for dendritic spine formation following initial axo-dendritic contact [3]. Unstable protospines are often referred as learning spines. As they mature, they acquire a mushroom shape that appears more stable

◀ **Fig. 8** Overexpression and downregulation of Exo70 alters recycling vesicles sites in hippocampal neurons. **a** Representative images showing EGFP (left panels) expression and FM 4–64 fluorescence (middle panels). Neuronal cultures were transduced with lentivirus expressing control-HA (upper panels) and Exo70FL (lower panels) at DIV 0 and FM 4–64 uptake was tested at DIV 15. First, neurons were depolarized as described in methods (Load) in the presence of FM 4–64. To unload, neurons were washed thoroughly with a second depolarization step. Images were obtained under load and unload conditions. Magnifications of dendrite section stained with FM 4–64 dye as shown as pseudocolor. Exocytosis ratio was calculated from FM 4–64 fluorescence intensity in load condition versus the fluorescence intensity in unload condition (load/unload intensities) (see upper graph). The amount of recycling vesicle sites was determined from the number of FM 4–64 puncta density after loading (see lower graph). **b** Representative images showing neuronal cultures transduced with Exo70-shRNA at 10 DIV and analyzed at DIV 15. Images were selected for measuring FM fluorescence intensities using region of interest areas (ROI) of 1.5 × 1.5 μm (**b**, **a`**, white arrow, pseudocolor to see recycling sites). ROI of the non-transfected dendritic tree were used as depolarization control with KCl (**b, b`**, red). **c** Graphs show unloading of the sites marked with FM 4–64 in neurons transfected with Exo70-sh-RNA (green; **a`**) and not transfected as control (red; **b`**). The number of sites marked with FM 4–64 per neurite length is shown in the graph to the right. Images were obtained using identical settings for laser power, confocal thickness, and detector sensitivity. All measures were carried at room temperature (25 °C). For the quantitation, 3 primary dendrites per neuron were used, $n = 8$ neurons per experiment. Each experimental group included 2 independent experiments. Values represent means ± SEM. ***$p < 0.005$. A.U.: arbitrary units

[74]. During this early phase, spine length is shortened, and spine head enlarges. Increases in spine volume are closely related to the accumulation of glutamate receptors [75] and the reorganization of the actin cytoskeleton within spines [76]. Accordingly, we found that Exo70 overexpression increased the number of mature spines and decreased the number of filopodia in mature neurons. Within dendritic spines, much of the overexpressed Exo70 was found at the spine head, while the endogenous protein, detected by specific antibodies, was localized within the spine shaft and head. The latter suggests that Exo70 might define spine domains to attract incoming vesicles with cargos. Exo70 increases the number of mature spines probably by regulating the delivery of functional important postsynaptic proteins including glutamate receptors [18, 75]. A cross-talk might occur among exocyst subunits at spines since Sec8 and Exo70 have been found to mediate the targeting and insertion of AMPA receptors, respectively [18]. Also, the delivery of NMDA receptors to the cell surface of neurons is mediated by Sec8 [77]. Another link between the exocyst and postsynapse formation has been recently described. In that study, the small GTPase Ral was shown to mediate synaptic activity with the recruitment of exocyst proteins to postsynaptic zones of the NMJ of *Drosophila*. The same was observed in cultured hippocampal neurons where activated Ra1A increased Sec5 in spines together with an increase in dendritic spine density [78]. Those observations and the data presented in the present work suggest a role of the exocyst in synaptic plasticity. A reorganization of the actin cytoskeleton might also be involved [76] as Exo70 is known to interact with Arp2/3 [31, 33] a protein complex which has been shown to modulate spine maturation [79].

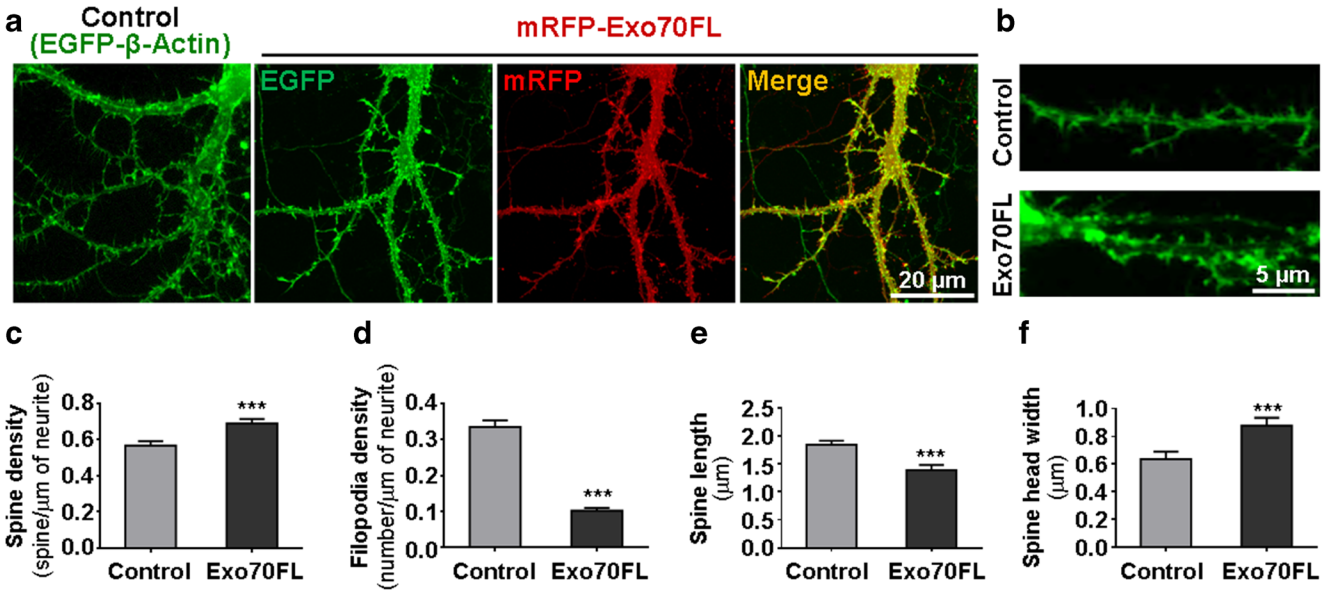

Fig. 9 Exo70FL overexpression promotes spine maturation in hippocampal neurons. **a** Representative images showing the expression of EGFP-β-Actin and mRFP-Exo70FL in primary neurons. Neuronal cultures were transduced at DIV 0 with monocistronic lentivirus FUR-Exo70-W and at DIV 1 with FUG-Actin-W expressing mRFP-Exo70 and EGFP-Actin, respectively and fixed at DIV 21. **b** Representative images of EGFP-β-Actin in control dendrites and after co-expression with mRFP-Exo70 showing an effect in spine number and morphology. **c** Quantification of dendritic spine density shown in (**a**) and (**b**). **d** Quantification of filopodia density shown in (**a**) and (**b**). **e** Quantification of length, and **f** head width of spines. All parameters were quantified in three primary dendrites per neuron. Each experimental group considered 2 independent experiments. Values represent means ± SEM, $n = 20$ neurons per experiment. ***$p < 0.005$

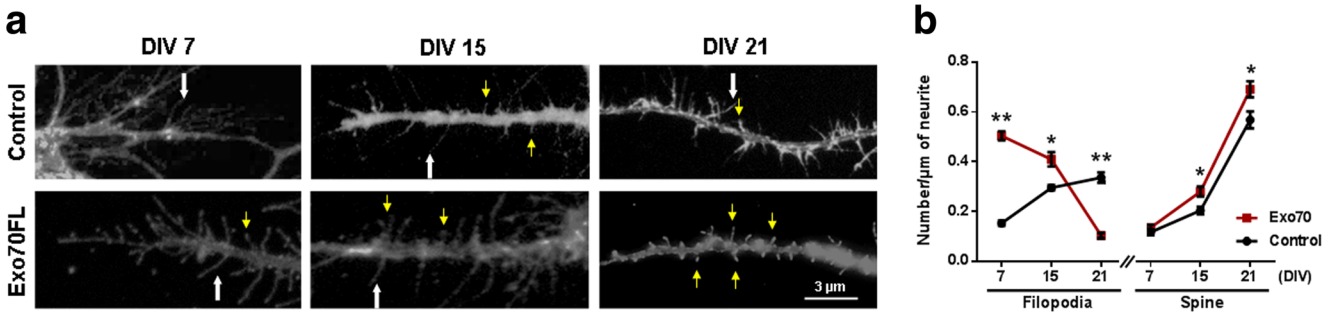

Fig. 10 Effect of Exo70 over-expression on the temporality of filopodia/spine maturation during neuronal development. **a** Hippocampal neurons were transduced at the day of plating (0 DIV) with bicistronic lentivirus expressing EGFP and Exo70FL, fixed and analyzed at DIV 7, 15, and 21 to quantified filopodia (white arrow) and spines development (yellow arrow), **b** graph showing the quantification of filopodia and spines at different days of cultures. Each experimental group considered 2 independent experiments. Values represent means ± SEM, $n = 20$ neurons per experiment. $^{*}p < 0.05$, $^{**}p < 0.005$

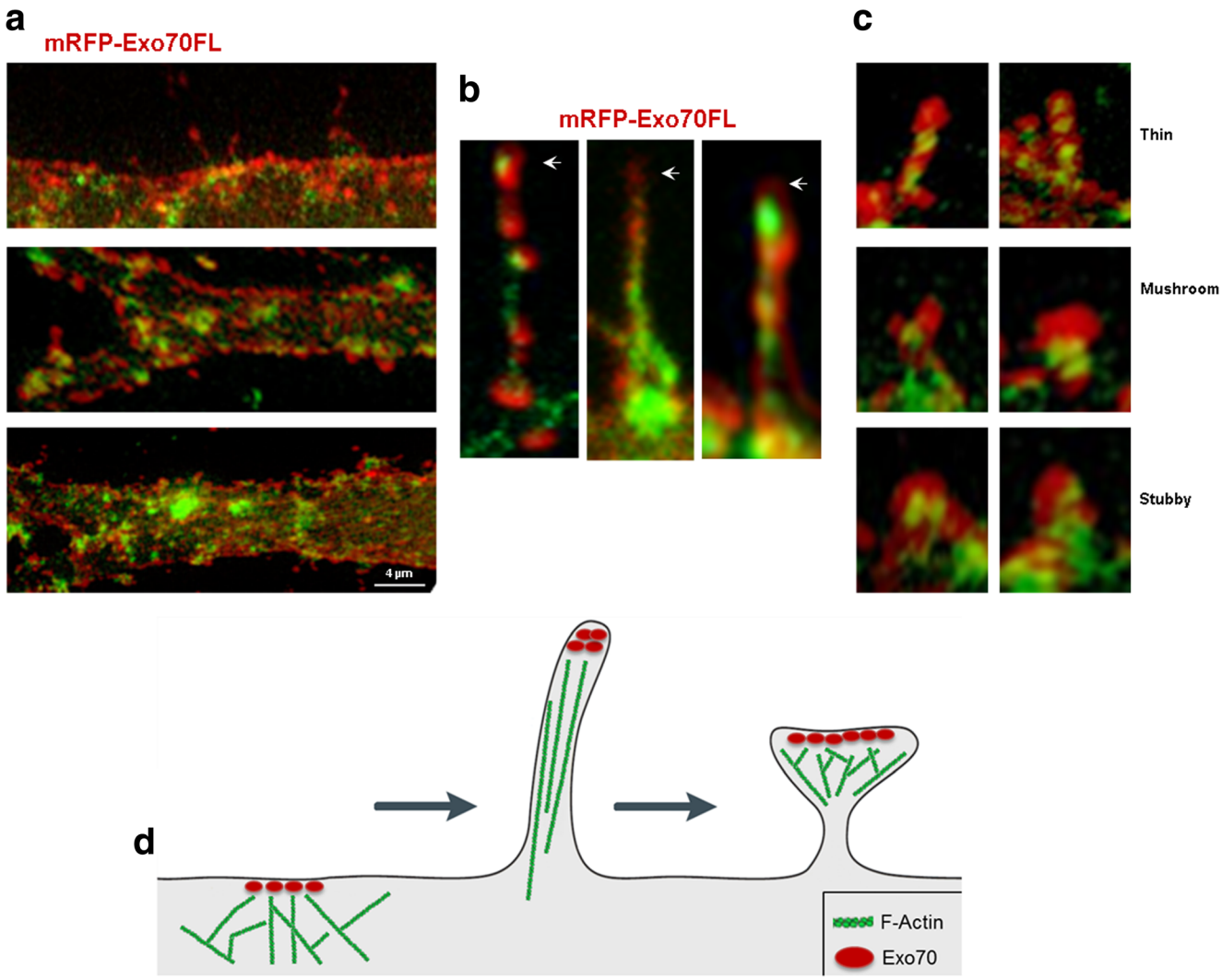

Fig. 11 Model proposed for the modulation of synaptogenesis and spines by Exo70. Representative super-resolution images taken at 21 DIV showing that Exo70 is associated with dendritic membranes (**a**), Exo70 is located at the tip of filopodia (**b**, white arrow head**),** and in dendritic spine heads (**c**). Examples show thin morphology (top), mushroom head shaped (mid) and stubby (bottom) spines. **d** Model proposed of Exo70 modulation of filopodia and spines at dendritic processes. The process is hypothesized to start with the recruitment of Exo70 to the plasma membrane and induce the formation of the filopodia. After filopodia find a synaptic companion they form a dynamic protospines. Subsequently, spines can mature in synaptically active neurons. Exo70 could be detected at all stages of spine maturation

Exo70 Role in Functional Synapses Density

The increase in dendrite branching and spine density was accompanied by a major synaptic puncta density of Piccolo, Shank3, and an increase in FM dye-labeled puncta, suggesting an increase in functional synaptic contacts. The number of synaptic proteins might also be modulated by Exo70 since at the level of individual synapses the intensity of Piccolo puncta, but not Shank3 increased slightly with Exo70 overexpression. Interestingly, shRNA-mediated knockdown of Exo70 decreased the density and intensity of synaptic puncta.

Additionally, the exocyst complex appears to extend its function to the presynapse as two exocyst subunit Sec6 and Sec8 were found associated with the tips of growing neurites, filopodia and growth cones [21], as well as within the presynaptic compartments [20], probably facilitating the delivery of vesicles to nascent active zones. When we analyzed neurons of DIV 21 by immunofluorescence with an antibody specific for Exo70, this protein besides being in dendrites and spines, showed an axonal dotted pattern that regularly colocalized with Bassoon. The presence of Exo70 in axons is not unexpected since a previous report showed the presence of Exo70 in an axonal growth cone preparation isolated from rat fetal brain [26]. In the latter study Exo70 together with TC10 play a role in membrane expansion regulated by IGF-1 in developing axons [26]. The presence and colocalization of Exo70 with Bassoon at mature presynapses are intriguing and our FM dye data suggest a role for this exocyst component in synaptic vesicle release, something interesting to explore in future studies. No further studies have addressed the presence of Exo70 at the presynapses of mature neurons.

Summarizing, the present findings position Exo70 in the group of proteins that modulate neuronal dendritic tree. As the presence of Exo70 appears to be both presynaptic and postsynaptic, the effect of Exo70 on dendrite arborization could be explained by its direct action in one of the synaptic compartments or in both. In one scenery, postsynaptic Exo70 might directly act on dendrite membrane expansion through its well-known role in vesicular membrane exocytosis. The latter situation is supported by the fact that Exo70 increased filopodia number in young DIV 7 hippocampal neurons, a period of low synaptic contacts. Another situation could be that pre- and postsynaptic Exo70 interacts directly with the machinery involved in the formation of active zones and postsynaptic densities, respectively, increasing the number of functional synapses and synaptic activity, what in turn will modulate the dendrite arbor [80–82]. Finally, the presence of Exo70 at the shaft and head of dendritic spines argues in favor of a direct role in the maturation of dendritic spines and a role in synaptic plasticity.

Funding Information This study was supported by grants from BMBF 20150065, FONDECYT 1110944, FONDECYT 1070462 and CODEI 3744 (Universidad de Antofagasta) to P.Z.; Basal Center of Excellence in Aging and Regeneration (CONICYT-PFB 12/2007), (AFB 170005) and FONDECYT N° 1160724 to N.C.I; Sociedad Química y Minera de Chile; Programa de Iniciación en Investigación para Investigadores Jóvenes de la Universidad de Antofagasta (D446-2015) and Convenio de Perfeccionamiento Académico de la Universidad de Antofagasta (D1109-2017) to P.R.O.

Compliance with Ethical Standards

Conflict of Interest The authors declare that they have no conflict of interest.

Ethical Approval All procedures performed in studies involving animal's participants were in accordance with the ethical standards of Universidad de Antofagasta research committee and Bioethical and Biosafety Committee of the Faculty of Biological Sciences of the Pontificia Universidad Católica de Chile approved the experimental procedures. The 1964 Helsinki declaration and its later amendments or comparable ethical standards. This article does not contain any studies with human participants performed by any of the authors.

References

1. Huttenlocher PR, Dabholkar AS (1997) Regional differences in synaptogenesis in human cerebral cortex. J Comp Neurol 387(2): 167–178
2. Vaughn JE, Barber RP, Sims TJ (1988) Dendritic development and preferential growth into synaptogenic fields: a quantitative study of Golgi-impregnated spinal motor neurons. Synapse 2(1):69–78. https://doi.org/10.1002/syn.890020110
3. Sekino Y, Kojima N, Shirao T (2007) Role of actin cytoskeleton in dendritic spine morphogenesis. Neurochem Int 51(2–4):92–104. https://doi.org/10.1016/j.neuint.2007.04.029
4. Zheng JQ, Wan JJ, Poo MM (1996) Essential role of filopodia in chemotropic turning of nerve growth cone induced by a glutamate gradient. J Neurosci 16(3):1140–1149
5. Ziv NE, Smith SJ (1996) Evidence for a role of dendritic filopodia in synaptogenesis and spine formation. Neuron 17(1):91–102
6. Waites CL, Craig AM, Garner CC (2005) Mechanisms of vertebrate synaptogenesis. Annu Rev Neurosci 28:251–274. https://doi.org/10.1146/annurev.neuro.27.070203.144336
7. Xu J, Luo F, Zhang Z, Xue L, Wu XS, Chiang HC, Shin W, Wu LG (2013) SNARE proteins synaptobrevin, SNAP-25, and syntaxin are involved in rapid and slow endocytosis at synapses. Cell Rep 3(5): 1414–1421. https://doi.org/10.1016/j.celrep.2013.03.010
8. Hutagalung AH, Novick PJ (2011) Role of Rab GTPases in membrane traffic and cell physiology. Physiol Rev 91(1):119–149. https://doi.org/10.1152/physrev.00059.2009
9. Wang T, Li L, Hong W (2017) SNARE proteins in membrane trafficking. Traffic 18(12):767–775. https://doi.org/10.1111/tra.12524
10. Mignogna ML, D'Adamo P (2017) Critical importance of RAB proteins for synaptic function. Small GTPases:1–13. https://doi.org/10.1080/21541248.2016.1277001
11. Lipschutz JH, Mostov KE (2002) Exocytosis: the many masters of the exocyst. Curr Biol 12(6):R212–R214
12. TerBush DR, Maurice T, Roth D, Novick P (1996) The exocyst is a multiprotein complex required for exocytosis in Saccharomyces cerevisiae. EMBO J 15(23):6483–6494

13. Heider MR, Munson M (2012) Exorcising the exocyst complex. Traffic 13(7):898–907. https://doi.org/10.1111/j.1600-0854.2012.01353.x
14. Wang H, Tang X, Liu J, Trautmann S, Balasundaram D, McCollum D, Balasubramanian MK (2002) The multiprotein exocyst complex is essential for cell separation in Schizosaccharomyces pombe. Mol Biol Cell 13(2):515–529. https://doi.org/10.1091/mbc.01-11-0542
15. Grindstaff KK, Yeaman C, Anandasabapathy N, Hsu SC, Rodriguez-Boulan E, Scheller RH, Nelson WJ (1998) Sec6/8 complex is recruited to cell-cell contacts and specifies transport vesicle delivery to the basal-lateral membrane in epithelial cells. Cell 93(5):731–740
16. Yeaman C, Grindstaff KK, Wright JR, Nelson WJ (2001) Sec6/8 complexes on trans-Golgi network and plasma membrane regulate late stages of exocytosis in mammalian cells. J Cell Biol 155(4):593–604. https://doi.org/10.1083/jcb.200107088
17. Sans N, Vissel B, Petralia RS, Wang YX, Chang K, Royle GA, Wang CY, O'Gorman S et al (2003) Aberrant formation of glutamate receptor complexes in hippocampal neurons of mice lacking the GluR2 AMPA receptor subunit. J Neurosci 23(28):9367–9373
18. Gerges NZ, Backos DS, Rupasinghe CN, Spaller MR, Esteban JA (2006) Dual role of the exocyst in AMPA receptor targeting and insertion into the postsynaptic membrane. EMBO J 25(8):1623–1634. https://doi.org/10.1038/sj.emboj.7601065
19. Inoue M, Chang L, Hwang J, Chiang SH, Saltiel AR (2003) The exocyst complex is required for targeting of Glut4 to the plasma membrane by insulin. Nature 422(6932):629–633. https://doi.org/10.1038/nature01533
20. Hazuka CD, Foletti DL, Hsu SC, Kee Y, Hopf FW, Scheller RH (1999) The sec6/8 complex is located at neurite outgrowth and axonal synapse-assembly domains. J Neurosci 19(4):1324–1334
21. Vega IE, Hsu SC (2001) The exocyst complex associates with microtubules to mediate vesicle targeting and neurite outgrowth. J Neurosci 21(11):3839–3848
22. Murthy M, Garza D, Scheller RH, Schwarz TL (2003) Mutations in the exocyst component Sec5 disrupt neuronal membrane traffic, but neurotransmitter release persists. Neuron 37(3):433–447
23. Peng Y, Lee J, Rowland K, Wen Y, Hua H, Carlson N, Lavania S, Parrish JZ et al (2015) Regulation of dendrite growth and maintenance by exocytosis. J Cell Sci 128(23):4279–4292. https://doi.org/10.1242/jcs.174771
24. Taylor CA, Yan J, Howell AS, Dong X, Shen K (2015) RAB-10 regulates dendritic branching by balancing dendritic transport. PLoS Genet 11(12):e1005695. https://doi.org/10.1371/journal.pgen.1005695
25. Zou W, Yadav S, DeVault L, Nung Jan Y, Sherwood DR (2015) RAB-10-dependent membrane transport is required for dendrite Arborization. PLoS Genet 11(9):e1005484. https://doi.org/10.1371/journal.pgen.1005484
26. Dupraz S, Grassi D, Bernis ME, Sosa L, Bisbal M, Gastaldi L, Jausoro I, Caceres A et al (2009) The TC10-Exo70 complex is essential for membrane expansion and axonal specification in developing neurons. J Neurosci 29(42):13292–13301. https://doi.org/10.1523/JNEUROSCI.3907-09.2009
27. Bodrikov V, Solis GP, Stuermer CA (2011) Prion protein promotes growth cone development through reggie/flotillin-dependent N-cadherin trafficking. J Neurosci 31(49):18013–18025. https://doi.org/10.1523/JNEUROSCI.4729-11.2011
28. Liu J, Zuo X, Yue P, Guo W (2007) Phosphatidylinositol 4,5-bisphosphate mediates the targeting of the exocyst to the plasma membrane for exocytosis in mammalian cells. Mol Biol Cell 18(11):4483–4492. https://doi.org/10.1091/mbc.E07-05-0461
29. Moore BA, Robinson HH, Xu Z (2007) The crystal structure of mouse Exo70 reveals unique features of the mammalian exocyst. J Mol Biol 371(2):410–421. https://doi.org/10.1016/j.jmb.2007.05.018
30. Hamburger ZA, Hamburger AE, West AP Jr, Weis WI (2006) Crystal structure of the S.cerevisiae exocyst component Exo70p. J Mol Biol 356(1):9–21. https://doi.org/10.1016/j.jmb.2005.09.099
31. Zuo X, Zhang J, Zhang Y, Hsu SC, Zhou D, Guo W (2006) Exo70 interacts with the Arp2/3 complex and regulates cell migration. Nat Cell Biol 8(12):1383–1388. https://doi.org/10.1038/ncb1505
32. Liu J, Yue P, Artym VV, Mueller SC, Guo W (2009) The role of the exocyst in matrix metalloproteinase secretion and actin dynamics during tumor cell invadopodia formation. Mol Biol Cell 20(16):3763–3771. https://doi.org/10.1091/mbc.E08-09-0967
33. Liu J, Zhao Y, Sun Y, He B, Yang C, Svitkina T, Goldman YE, Guo W (2012) Exo70 stimulates the Arp2/3 complex for lamellipodia formation and directional cell migration. Curr Biol 22(16):1510–1515. https://doi.org/10.1016/j.cub.2012.05.055
34. Torres V, Barra L, Garces F, Ordenes K, Leal-Ortiz S, Garner CC, Fernandez F, Zamorano P (2010) A bicistronic lentiviral vector based on the 1D/2A sequence of foot-and-mouth disease virus expresses proteins stoichiometrically. J Biotechnol 146(3):138–142. https://doi.org/10.1016/j.jbiotec.2010.01.017
35. Reynolds A, Leake D, Boese Q, Scaringe S, Marshall WS, Khvorova A (2004) Rational siRNA design for RNA interference. Nat Biotechnol 22(3):326–330. https://doi.org/10.1038/nbt936
36. Ui-Tei K, Naito Y, Takahashi F, Haraguchi T, Ohki-Hamazaki H, Juni A, Ueda R, Saigo K (2004) Guidelines for the selection of highly effective siRNA sequences for mammalian and chick RNA interference. Nucleic Acids Res 32(3):936–948. https://doi.org/10.1093/nar/gkh247
37. Yoshinari K, Miyagishi M, Taira K (2004) Effects on RNAi of the tight structure, sequence and position of the targeted region. Nucleic Acids Res 32(2):691–699. https://doi.org/10.1093/nar/gkh221
38. Taxman DJ, Livingstone LR, Zhang J, Conti BJ, Iocca HA, Williams KL, Lich JD, Ting JP et al (2006) Criteria for effective design, construction, and gene knockdown by shRNA vectors. BMC Biotechnol 6:7. https://doi.org/10.1186/1472-6750-6-7
39. Leal-Ortiz S, Waites CL, Terry-Lorenzo R, Zamorano P, Gundelfinger ED, Garner CC (2008) Piccolo modulation of Synapsin1a dynamics regulates synaptic vesicle exocytosis. J Cell Biol 181(5):831–846. https://doi.org/10.1083/jcb.200711167
40. Fernandez A, Guzman S, Cruz Y, Zamorano P (2014) Construction of bicistronic lentiviral vectors for tracking the expression of CDNF in transduced cells. Plasmid 76:15–23. https://doi.org/10.1016/j.plasmid.2014.09.001
41. Kaech S, Banker G (2006) Culturing hippocampal neurons. Nat Protoc 1(5):2406–2415. https://doi.org/10.1038/nprot.2006.356
42. Lois C, Hong EJ, Pease S, Brown EJ, Baltimore D (2002) Germline transmission and tissue-specific expression of transgenes delivered by lentiviral vectors. Science 295(5556):868–872. https://doi.org/10.1126/science.1067081
43. Cerpa W, Godoy JA, Alfaro I, Farias GG, Metcalfe MJ, Fuentealba R, Bonansco C, Inestrosa NC (2008) Wnt-7a modulates the synaptic vesicle cycle and synaptic transmission in hippocampal neurons. J Biol Chem 283(9):5918–5927. https://doi.org/10.1074/jbc.M705943200
44. Smalla K-H, Klemmer P, Wyneken U (2013) Isolation of the postsynaptic density: a specialization of the subsynaptic cytoskeleton #. In: T the cytoskeleton, vol 79. Neuromethods. pp 265–280
45. Tsuriel S, Geva R, Zamorano P, Dresbach T, Boeckers T, Gundelfinger ED, Garner CC, Ziv NE (2006) Local sharing as a predominant determinant of synaptic matrix molecular dynamics. PLoS Biol 4(9):e271. https://doi.org/10.1371/journal.pbio.0040271
46. Peters A, Kaiserman-Abramof IR (1970) The small pyramidal neuron of the rat cerebral cortex. The perikaryon, dendrites and spines. Am J Anat 127(4):321–355. https://doi.org/10.1002/aja.1001270402

47. Berry KP, Nedivi E (2017) Spine dynamics: are they all the same? Neuron 96(1):43–55. https://doi.org/10.1016/j.neuron.2017.08.008
48. Wang S, Liu Y, Adamson CL, Valdez G, Guo W, Hsu SC (2004) The mammalian exocyst, a complex required for exocytosis, inhibits tubulin polymerization. J Biol Chem 279(34):35958–35966. https://doi.org/10.1074/jbc.M313778200
49. Zhao Y, Liu J, Yang C, Capraro BR, Baumgart T, Bradley RP, Ramakrishnan N, Xu X et al (2013) Exo70 generates membrane curvature for morphogenesis and cell migration. Dev Cell 26(3): 266–278. https://doi.org/10.1016/j.devcel.2013.07.007
50. Sholl DA (1953) Dendritic organization in the neurons of the visual and motor cortices of the cat. J Anat 87(4):387–406
51. Cline HT (2001) Dendritic arbor development and synaptogenesis. Curr Opin Neurobiol 11(1):118–126
52. Suzuki T (2011) Isolation of synapse subdomains by subcellular fractionation using sucrose density gradient centrifugation. In: Li KW (ed) Neuroproteomics. Humana Press, Totowa, pp. 47–61. https://doi.org/10.1007/978-1-61779-111-6_4
53. Bresler T, Ramati Y, Zamorano PL, Zhai R, Garner CC, Ziv NE (2001) The dynamics of SAP90/PSD-95 recruitment to new synaptic junctions. Mol Cell Neurosci 18(2):149–167. https://doi.org/10.1006/mcne.2001.1012
54. Wu B, Guo W (2015) The exocyst at a glance. J Cell Sci 128(16): 2957–2964. https://doi.org/10.1242/jcs.156398
55. Minerbi A, Kahana R, Goldfeld L, Kaufman M, Marom S, Ziv NE (2009) Long-term relationships between synaptic tenacity, synaptic remodeling, and network activity. PLoS Biol 7(6):e1000136. https://doi.org/10.1371/journal.pbio.1000136
56. Jan YN, Jan LY (2010) Branching out: mechanisms of dendritic arborization. Nat Rev Neurosci 11(5):316–328. https://doi.org/10.1038/nrn2836
57. Aizawa H, Hu SC, Bobb K, Balakrishnan K, Ince G, Gurevich I, Cowan M, Ghosh A (2004) Dendrite development regulated by CREST, a calcium-regulated transcriptional activator. Science 303(5655):197–202. https://doi.org/10.1126/science.1089845
58. Gaudilliere B, Konishi Y, de la Iglesia N, Yao G, Bonni A (2004) A CaMKII-NeuroD signaling pathway specifies dendritic morphogenesis. Neuron 41(2):229–241
59. McAllister AK, Lo DC, Katz LC (1995) Neurotrophins regulate dendritic growth in developing visual cortex. Neuron 15(4):791–803
60. Rosso SB, Sussman D, Wynshaw-Boris A, Salinas PC (2005) Wnt signaling through Dishevelled, Rac and JNK regulates dendritic development. Nat Neurosci 8(1):34–42. https://doi.org/10.1038/nn1374
61. Hoogenraad CC, Milstein AD, Ethell IM, Henkemeyer M, Sheng M (2005) GRIP1 controls dendrite morphogenesis by regulating EphB receptor trafficking. Nat Neurosci 8(7):906–915. https://doi.org/10.1038/nn1487
62. Morita A, Yamashita N, Sasaki Y, Uchida Y, Nakajima O, Nakamura F, Yagi T, Taniguchi M et al (2006) Regulation of dendritic branching and spine maturation by semaphorin3A-Fyn signaling. J Neurosci 26(11):2971–2980. https://doi.org/10.1523/JNEUROSCI.5453-05.2006
63. Komiyama T, Sweeney LB, Schuldiner O, Garcia KC, Luo L (2007) Graded expression of semaphorin-1a cell-autonomously directs dendritic targeting of olfactory projection neurons. Cell 128(2):399–410. https://doi.org/10.1016/j.cell.2006.12.028
64. Newey SE, Velamoor V, Govek EE, Van Aelst L (2005) Rho GTPases, dendritic structure, and mental retardation. J Neurobiol 64(1):58–74. https://doi.org/10.1002/neu.20153
65. Leemhuis J, Boutillier S, Barth H, Feuerstein TJ, Brock C, Nurnberg B, Aktories K, Meyer DK (2004) Rho GTPases and phosphoinositide 3-kinase organize formation of branched dendrites. J Biol Chem 279(1):585–596. https://doi.org/10.1074/jbc.M307066200
66. Lee A, Li W, Xu K, Bogert BA, Su K, Gao FB (2003) Control of dendritic development by the Drosophila fragile X-related gene involves the small GTPase Rac1. Development 130(22):5543–5552. https://doi.org/10.1242/dev.00792
67. Zheng Y, Wildonger J, Ye B, Zhang Y, Kita A, Younger SH, Zimmerman S, Jan LY et al (2008) Dynein is required for polarized dendritic transport and uniform microtubule orientation in axons. Nat Cell Biol 10(10):1172–1180. https://doi.org/10.1038/ncb1777
68. Ye B, Zhang Y, Song W, Younger SH, Jan LY, Jan YN (2007) Growing dendrites and axons differ in their reliance on the secretory pathway. Cell 130(4):717–729. https://doi.org/10.1016/j.cell.2007.06.032
69. Satoh D, Sato D, Tsuyama T, Saito M, Ohkura H, Rolls MM, Ishikawa F, Uemura T (2008) Spatial control of branching within dendritic arbors by dynein-dependent transport of Rab5-endosomes. Nat Cell Biol 10(10):1164–1171. https://doi.org/10.1038/ncb1776
70. Marrs GS, Green SH, Dailey ME (2001) Rapid formation and remodeling of postsynaptic densities in developing dendrites. Nat Neurosci 4(10):1006–1013. https://doi.org/10.1038/nn717
71. Portera-Cailliau C, Pan DT, Yuste R (2003) Activity-regulated dynamic behavior of early dendritic protrusions: evidence for different types of dendritic filopodia. J Neurosci 23(18):7129–7142
72. Yoshihara Y, De Roo M, Muller D (2009) Dendritic spine formation and stabilization. Curr Opin Neurobiol 19(2):146–153. https://doi.org/10.1016/j.conb.2009.05.013
73. Mattison HA, Popovkina D, Kao JP, Thompson SM (2014) The role of glutamate in the morphological and physiological development of dendritic spines. Eur J Neurosci 39(11):1761–1770. https://doi.org/10.1111/ejn.12536
74. Bourne JN, Harris KM (2008) Balancing structure and function at hippocampal dendritic spines. Annu Rev Neurosci 31:47–67. https://doi.org/10.1146/annurev.neuro.31.060407.125646
75. Zito K, Scheuss V, Knott G, Hill T, Svoboda K (2009) Rapid functional maturation of nascent dendritic spines. Neuron 61(2):247–258. https://doi.org/10.1016/j.neuron.2008.10.054
76. Honkura N, Matsuzaki M, Noguchi J, Ellis-Davies GC, Kasai H (2008) The subspine organization of actin fibers regulates the structure and plasticity of dendritic spines. Neuron 57(5):719–729. https://doi.org/10.1016/j.neuron.2008.01.013
77. Sans N, Prybylowski K, Petralia RS, Chang K, Wang YX, Racca C, Vicini S, Wenthold RJ (2003) NMDA receptor trafficking through an interaction between PDZ proteins and the exocyst complex. Nat Cell Biol 5(6):520–530. https://doi.org/10.1038/ncb990
78. Teodoro RO, Pekkurnaz G, Nasser A, Higashi-Kovtun ME, Balakireva M, McLachlan IG, Camonis J, Schwarz TL (2013) Ral mediates activity-dependent growth of postsynaptic membranes via recruitment of the exocyst. EMBO J 32(14):2039–2055. https://doi.org/10.1038/emboj.2013.147
79. Spence EF, Kanak DJ, Carlson BR, Soderling SH (2016) The Arp2/3 complex is essential for distinct stages of spine synapse maturation, including synapse unsilencing. J Neurosci 36(37):9696–9709. https://doi.org/10.1523/JNEUROSCI.0876-16.2016
80. Parrish JZ, Emoto K, Kim MD, Jan YN (2007) Mechanisms that regulate establishment, maintenance, and remodeling of dendritic fields. Annu Rev Neurosci 30:399–423. https://doi.org/10.1146/annurev.neuro.29.051605.112907
81. Wong RO, Ghosh A (2002) Activity-dependent regulation of dendritic growth and patterning. Nat Rev Neurosci 3(10):803–812. https://doi.org/10.1038/nrn941
82. Peng YR, He S, Marie H, Zeng SY, Ma J, Tan ZJ, Lee SY, Malenka RC et al (2009) Coordinated changes in dendritic arborization and synaptic strength during neural circuit development. Neuron 61(1): 71–84. https://doi.org/10.1016/j.neuron.2008.11.015